SIAM J. NUMER. ANAL.
Vol. 54, No. 5, pp. 2910–2937

ON THE RATE OF CONVERGENCE OF FLUX RECONSTRUCTION FOR STEADY-STATE PROBLEMS*

KARTIKEY ASTHANA†, JERRY WATKINS†, AND ANTONY JAMESON†

Abstract. This paper derives analytical estimates for the rates of convergence of numerical first and second derivative operators involved in flux reconstruction (FR). These estimates yield the rate of convergence for steady-state advection-diffusion problems when error is measured in the vector seminorm induced by the advection-diffusion operator. This serves to rigorously quantify the effect of polynomial order, correction functions, and upwinding coefficients on the accuracy of FR schemes. We prove that for centered fluxes, the derivative operator exhibits superconvergence for a special class of correction functions, designated "SFR," which includes the nodal DG scheme. Finally, we also show that the rate of convergence of the vector ℓ^2 norm of error for such steady-state problems is identical to the short-time rate of convergence for time-dependent problems derived in [K. Asthana et al., *Analysis and Design of Optimal Discontinuous Finite Element Schemes*, Ph.D. thesis, Stanford University, Stanford, CA, 2016].

Key words. flux reconstruction, discontinuous Galerkin, high-order, steady state, rate of convergence, derivative operator

AMS subject classifications. 65N12, 65N15, 65N30, 65M70

DOI. 10.1137/16M1055682

1. Introduction.

The discontinuous Galerkin (DG) formulation provides a computationally tractable, high-order, unstructured approach to tackle conservation laws arising in a wide range of applications ranging from computational mechanics [14] to stochastic control [10]. A salient feature of this method is that it exhibits superconvergence in nodal [1], functional [11, 12], as well as spectral [2, 3] points of view. In regard to linear, time-dependent problems, Cheng and Shu [12] have studied the grid-convergence of error for a DG scheme with polynomial order P using upwinded fluxes on arbitrary meshes. The authors show that the evolution of the L^2 norm of error is bounded by a linear function of time where the constant term converges at the order $P+1$, and the linear term converges at the order $P+3/2$. Hence, the rate of convergence at short-time, $t = 0^+$, is different from that at long-time, $t \to \infty$. A similar investigation was conducted in [6] for the flux reconstruction (FR) formulation [16, 17] wherein Fourier analysis was utilized to derive the rate of convergence of error at the set of solution points. It was proven that the short-time rate of convergence depends on the convergence-rates of the modal weights for the "spurious" modes, and the long-time rate depends on the convergence-rate of the "physical" eigenvalue. Table 1 records these rates for the DG scheme, recovered via FR, for upwinded and centered fluxes, and odd and even P. In an analogous manner, rates can be determined for any stable scheme within the FR family.

The long-time superconvergence rate is valuable for time-dependent problems, especially when the long-time solution is independent of the initial condition [7].

*Received by the editors March 11, 2016; accepted for publication (in revised form) July 1, 2016; published electronically September 27, 2016.

http://www.siam.org/journals/sinum/54-5/M105568.html

Funding: The work of the first author was supported by the Thomas V. Jones Stanford Graduate Fellowship. The work of the second author was supported by the National Science Foundation Graduate Research Fellowship Program.

†Department of Aeronautics and Astronautics, Stanford University, Stanford, CA 94305 (kasthana@stanford.edu, watkins2@stanford.edu, jameson@baboon.stanford.edu).

TABLE 1
Rate of convergence at the set of solution points for the DG scheme of polynomial order P, recovered via FR, for linear, time-dependent problems [6].

DG scheme	Short-time $t = 0^+$	Long-time $t \to \infty$
one-sided fluxes	$P+1$	$2P+1$
centered fluxes and even P	$P+2$	$2P+2$
centered fluxes and odd P	P	$2P$

However, it is not obvious whether such superconvergence extends to steady-state problems which routinely appear in aerospace and automobile design applications [18]. In fact, canonical test problems for evaluating numerical schemes are often based on the steady Euler and Navier–Stokes equations. For the DG scheme, several a posteriori error estimates [8, 19] exist for elliptic problems. Arnold et al. [4] provide a comprehensive comparison of several DG type methods, showing that the L^2 norm of the solution converges at the order $P+1$, while the H^1 norm converges at the order P. Similar observations were made by Williams et al. [20] for Couette flow using DG recovered via FR. Similarly, Cockburn et al. [13] have derived a priori error estimates for the Poisson equation on tensor-product elements. The authors show that, with the choice of a special numerical flux, the L^2 norm of the solution converges at the order $P+1$, while that of the derivative converges at $P+1/2$.

In this paper, we derive estimates for the rate of convergence of FR for a forced, linear, advection-diffusion problem having a steady-state. Two different measures of error are investigated. For the vector ℓ^2 norm, which measures pointwise error over the set of solution points, we show that the rate of convergence is identical to the short-time rate of convergence for time-dependent problems recorded in Table 1. We also measure error with respect to the vector seminorm induced by the advection-diffusion operator, and show that convergence in this measure depends on the rate of convergence of the numerical derivative operators involved in FR. Estimates are derived for error in the first and second derivative operators as a function of polynomial order, correction functions, and upwinding coefficients. This analysis has led to the prescription of a new class of superconvergent schemes, discussed in section 3.4, within the FR family which includes DG as a special case.

This paper is formatted as follows. In section 2, we describe the model problem and introduce the two measures of error, viz. the $\ell^2(\Omega^\delta)$ norm and the $\mathcal{L}^\delta(\Omega^\delta)$ seminorm. Section 3 then derives the rates of convergence of the numerical first and second derivative operators involved in FR. The main results are summarized in Theorems 3.5 and 3.7. These results allow us to obtain the rate of convergence of the numerical solution in the $\mathcal{L}^\delta(\Omega^\delta)$ seminorm, expressed in Corollary 3.8. In section 4, we use results from [6] to express error in terms of the asymptotic eigensolution. This leads to Theorem 4.3 which provides the rate of convergence of the numerical solution in the $\ell^2(\Omega)$ norm. The paper ends with section 5, where we perform simple numerical experiments to verify the derived results.

2. Error in numerical solution of steady advection-diffusion. This section derives an equation for error in the FR solution of a forced, scalar, advection-diffusion equation which exhibits a steady-state. We define two discrete measures of error that are utilized in the rest of this paper. Our first result shows that the rate of convergence of error, with respect to the seminorm induced by the advection-diffusion operator, is directly dependent on the rates of convergence of numerical spatial derivative opera-

tors in FR.

2.1. Problem specification. Consider the linear advection-diffusion equation in one dimension for a scalar-valued function, $\hat{u} \in \left(\mathbb{C}^2((0,1)) \times \mathbb{C}^1(\mathbb{R}_{++})\right)$, driven by a steady, sinusoidal forcing term of wavenumber $k = 2\pi m,\ m \in \mathbb{N}$,

$$\frac{\partial \hat{u}}{\partial t}(x,t) + (\mathcal{L}\hat{u})(x,t) = (iak + bk^2)\exp(ikx), \quad x \in (0,1),\ t > 0, \tag{2.1}$$

$$\hat{u}(x,0) = \exp(ik_0 x), \quad x \in [0,1], \tag{2.2}$$

$$\frac{\partial^r \hat{u}}{\partial x^r}(0,t) = \frac{\partial^r \hat{u}}{\partial x^r}(1,t), \quad r = 0,1, \ \ t \geq 0, \tag{2.3}$$

$$\mathcal{L} := a\frac{\partial}{\partial x} - b\frac{\partial^2}{\partial x^2}, \tag{2.4}$$

where $k_0 = 2\pi m_0,\ m_0 \in \mathbb{N}$ is the wavenumber of the initial condition, and $a \in \mathbb{R}_+, b \in \mathbb{R}_{++}$ are advection and diffusion coefficients, respectively. The boundary conditions are assumed to be periodic for simplicity. The analytical solution to (2.1)–(2.4) for $x \in [0,1],\ t \geq 0$, is given by

$$\hat{u}(x,t) = \exp\left(ik_0(x-at) - bk_0^2 t\right) + \exp(ikx)\left[1 - \exp\left(-iakt - bk^2 t\right)\right], \tag{2.5}$$

where the first term corresponds to the exponential decay of the initial condition and the second one corresponds to the growth of the particular solution driven by the source. Since $k_0 \neq 0$, the initial sinusoid is guaranteed to vanish as $t \to \infty$, resulting in the steady-state with wavenumber k. The corresponding rate of decay is dictated by the magnitude of k_0. In the special case of $k_0 = k$, the initial condition is itself steady.

Restriction of the problem to twice continuously differentiable functions allows for numerical procedures that attempt to approximate (2.1) directly in strong form. In the case of FR, the domain $\Omega = [0,1]$ is partitioned into nonoverlapping segments $\Omega = \bigcup_{n=1}^{N} \Omega_n$. For a scheme of order P, each segment is further discretized with $P+1$ distinct solution points Ω_n^δ. The numerical solution, $\hat{u}^\delta$, when restricted to Ω_n, resides within a polynomial space $\mathbb{P}_P(\Omega_n)$ consisting of all polynomials of degree P or lower. The numerical conservation law is obtained by satisfying (2.1) at the set of solution points, $\Omega^\delta = \bigcup_{n=1}^{N} \Omega_n^\delta$,

$$\frac{\partial^\delta \hat{u}^\delta}{\partial t}(x,t) + (\mathcal{L}^\delta \hat{u}^\delta)(x,t) = (iak + bk^2)\exp(ikx), \quad x \in \Omega^\delta,\ t > 0, \tag{2.6}$$

$$\hat{u}^\delta(x,0) = (\mathcal{P}\hat{u}_0)(x), \quad x \in [0,1], \tag{2.7}$$

$$\frac{\partial^r \hat{u}^\delta}{\partial x^r}(0,t) = \frac{\partial^r \hat{u}^\delta}{\partial x^r}(1,t), \quad r = 0,1, \ \ t \geq 0, \tag{2.8}$$

$$\mathcal{L}^\delta := a\frac{\partial^\delta}{\partial x} - b\frac{\partial^\delta}{\partial x}\frac{\partial^\delta}{\partial x}, \tag{2.9}$$

where $\mathcal{L}^\delta$ is the numerical differentiation operator in space and $\frac{\partial^\delta}{\partial t}$ is that in time, $\hat{u}_0(x) = \exp(ik_0 x)$ is the initial condition for the exact problem, and $\mathcal{P}$ is the collocation-projection operator that maps the initial condition to the space of the numerical solution. The primary quantity of interest is the error in the numerical solution,

$$e_{\hat{u}}(x,t) := \hat{u}^\delta(x,t) - \hat{u}(x,t), \quad x \in [0,1],\ t \geq 0. \tag{2.10}$$

A governing equation for the dynamics of error can be obtained by subtracting (2.1)–(2.3) from (2.6)–(2.8) and adding and subtracting terms, so that after algebraic rearrangement we obtain

(2.11)
$$\frac{\partial^\delta e_{\hat{u}}}{\partial t}(x,t) + (\mathcal{L}^\delta e_{\hat{u}})(x,t) = \left[\left(\frac{\partial}{\partial t} - \frac{\partial^\delta}{\partial t}\right) + (\mathcal{L} - \mathcal{L}^\delta)\right]\hat{u}(x,t), \quad x \in \Omega^\delta,\ t > 0,$$

$$e_{\hat{u}}(x,0) = (\mathcal{P}\hat{u}_0)(x) - \hat{u}_0(x), \quad x \in [0,1], \tag{2.12}$$

$$\frac{\partial^r e_{\hat{u}}}{\partial x^r}(0,t) = \frac{\partial^r e_{\hat{u}}}{\partial x^r}(1,t), \quad r = 0,1,\ \ t \geq 0, \tag{2.13}$$

which shows that the error itself follows a modified form of the numerical conservation law which is driven by the error in the differentiation operators in space and time. At time $t = 0$, the error is solely on account of the projection of the initial condition onto the space of the numerical solution. Thereafter, it is driven by the inability of the scheme to accurately differentiate the exact solution.

2.2. Error in steady-state solution. The evolution of pointwise error in time was investigated in [6] using Fourier analysis. We are now interested in the rate of convergence of error for a conservation law exhibiting a steady-state. Towards this end, let u be the unique limit $u(x) := \lim_{t\to\infty} \hat{u}(x,t) = \exp(ikx)$ which satisfies the steady advection-diffusion equation,

$$(\mathcal{L}u)(x) = (iak + bk^2)\exp(ikx), \quad x \in (0,1), \tag{2.14}$$

$$\frac{\partial^r u}{\partial x^r}(0) = \frac{\partial^r u}{\partial x^r}(1), \quad r = 0,1, \tag{2.15}$$

a periodic problem on the unit interval. Similarly, for any stable and consistent numerical scheme, let u^δ be the limit $u^\delta(x) := \lim_{t\to\infty} \hat{u}^\delta(x,t)$ which must satisfy

$$(\mathcal{L}^\delta u^\delta)(x) = (iak + bk^2)\exp(ikx), \quad x \in \Omega^\delta, \tag{2.16}$$

$$\frac{\partial^r u^\delta}{\partial x^r}(0) = \frac{\partial^r u^\delta}{\partial x^r}(1), \quad r = 0,1. \tag{2.17}$$

Existence and uniqueness of u^δ, in the limit of asymptotic grid resolution, follows from the proof of convergence [6] for linear, time-dependent problems. Heuristically, this is expected since $\hat{u}^\delta(x,t) \to \hat{u}(x,t)$ for $x \in [0,1]$, at any time $t > 0$. Also, on account of uniqueness, the limit is independent of the time integration scheme implied by the temporal discretization operator $\frac{\partial^\delta}{\partial t}$.

With these observations in place, we see from (2.11)–(2.17) that the pointwise error also exhibits a unique limit,

$$e_u(x) := \lim_{t\to\infty} e_{\hat{u}}(x,t) = u^\delta(x) - u(x) = u^\delta(x) - \exp(ikx), \quad x \in [0,1], \tag{2.18}$$

which satisfies

$$(\mathcal{L}^\delta e_u)(x) = (\mathcal{L} - \mathcal{L}^\delta)\exp(ikx), \quad x \in \Omega^\delta, \tag{2.19}$$

$$\frac{\partial^r e_u}{\partial x^r}(0) = \frac{\partial^r e_u}{\partial x^r}(1), \quad r = 0,1, \tag{2.20}$$

which is a discrete Poisson equation with a forcing term equal to the difference between the true derivative $\mathcal{L}u$ and the numerical derivative $\mathcal{L}^\delta u$ of the exact solution,

$$(\mathcal{L} - \mathcal{L}^\delta)\exp(ikx) = \left[a\left(ik - \frac{\partial^\delta}{\partial x}\right) + b\left(k^2 + \frac{\partial^\delta \partial^\delta}{\partial x \partial x}\right)\right]\exp(ikx), \quad x \in \Omega^\delta. \tag{2.21}$$

2.3. Measures of error. In this paper, we utilize two different measures of error. Traditionally, finite element schemes have been analyzed through the use of functional norms, especially of the Sobolev type which integrate error and its derivatives across the domain. However, owing to the nodal nature of FR, both of our employed measures are discrete in nature, and accumulate over the set of solution points. We define the vector ℓ^2 norm of error over the set of solution points as

$$\|e_u\|_{\ell^2(\Omega^\delta)} := \left[\frac{1}{N(P+1)}\sum_{n=1}^{N}\sum_{p=1}^{P+1}|e_u(x_{n,p})|^2\right]^{1/2}, \tag{2.22}$$

where $x_{n,p}$ is the pth solution point in the nth element. The rate of convergence of error with respect to this norm is derived in section 4.

In order to obtain the second measure, consider the seminorm which is induced by the advection-diffusion operator,

$$\|e_u\|_{\mathcal{L}^\delta(\Omega^\delta)} = \left[\frac{1}{N(P+1)}\sum_{n=1}^{N}\sum_{p=1}^{P+1}\left|(\mathcal{L}^\delta e_u)(x_{n,p})\right|^2\right]^{1/2}, \tag{2.23}$$

where $\mathcal{L}^\delta$ is as defined in (2.9). The requirements of nonnegativity and triangle inequality follow from the fact that $\|e_u\|_{\mathcal{L}^\delta(\Omega^\delta)} = \|\mathcal{L}^\delta e_u\|_{\ell^2(\Omega^\delta)}$ and that $\mathcal{L}^\delta$ is a linear operator. Let $h := \min_{n=1}^{N}|\Omega_n|$ be the length of the smallest element in the domain. Then, owing to the consistency of the FR formulation, we are guaranteed that $\exists\ \sigma^{(1)} > 0$, $\sigma^{(2)} > 0$ such that

$$\lim_{h\to 0}\left|\left(\frac{\partial^\delta}{\partial x} - ik\right)\exp(ikx)\right| \le c(k,P)\ h^{\sigma^{(1)}}, \tag{2.24}$$

$$\lim_{h\to 0}\left|\left(\frac{\partial^\delta \partial^\delta}{\partial x \partial x} + k^2\right)\exp(ikx)\right| \le c(k,P)\ h^{\sigma^{(2)}} \tag{2.25}$$

for all wavenumbers k, and $x \in \Omega^\delta$. Here $c > 0$ is some (k,P)-dependent constant and $\sigma^{(1)}$ and $\sigma^{(2)}$ denote the orders at which the first and second order numerical derivatives converge to the exact derivatives, respectively. The rate of convergence of error in $\mathcal{L}^\delta$ can now be obtained by substituting (2.19), (2.21), (2.24)–(2.25) into (2.23),

$$\begin{aligned}
\|e_u\|_{\mathcal{L}^\delta(\Omega^\delta)} &= \left\|(\mathcal{L}-\mathcal{L}^\delta)\exp(ikx)\right\|_{\ell^2(\Omega^\delta)} \\
&= \left\|\left[a\left(ik - \frac{\partial^\delta}{\partial x}\right) + b\left(k^2 + \frac{\partial^\delta \partial^\delta}{\partial x \partial x}\right)\right]\exp(ikx)\right\|_{\ell^2(\Omega^\delta)} \\
&\le |a|\left\|\left(ik - \frac{\partial^\delta}{\partial x}\right)\exp(ikx)\right\|_{\ell^2(\Omega^\delta)} + b\left\|\left(k^2 + \frac{\partial^\delta \partial^\delta}{\partial x \partial x}\right)\exp(ikx)\right\|_{\ell^2(\Omega^\delta)} \\
&\le |a|\max_{x\in\Omega^\delta}\left|\left(ik - \frac{\partial^\delta}{\partial x}\right)\exp(ikx)\right| + b\max_{x\in\Omega^\delta}\left|\left(k^2 + \frac{\partial^\delta \partial^\delta}{\partial x \partial x}\right)\exp(ikx)\right| \\
&\le c(k,P)\left[|a|h^{\sigma^{(1)}} + bh^{\sigma^{(2)}}\right] \quad \text{as } h \to 0.
\end{aligned} \tag{2.26}$$

This shows that the rate of convergence of error in the $\mathcal{L}^\delta$ seminorm is directly dependent on the rates of convergence of the numerical first and second derivative operators. The utility of this result lies in the fact that derivative operators in FR are analytically tractable as demonstrated in the next section.

3. Rates of convergence for derivative operators in FR. This section quantifies the error in the first and second order derivative operators involved in FR. We show that, for an FR scheme of polynomial order P, the order of convergence of the first derivative operator depends on whether P is odd or even. For odd P, the order is exactly P. For even P, the order can be $P+1$ under special conditions on the correction function and upwinding coefficient. These special conditions are satisfied by a family of linearly stable schemes with $P/2$ parameters. The nodal DG scheme with centered fluxes is also recovered as a member of this family. The order of convergence of the second derivative operator is dependent on the orders of convergence of constituent first derivative operators.

3.1. Derivative operators in flux reconstruction. We begin by providing a quick overview of the FR formulation for evaluating the numerical derivative of a smooth function. A detailed account of the reconstruction procedure can be found in [16, 17, 9].

Continuing our discussion from section 2, consider a set of equispaced nodes on the domain such that $x_1 = 0$, $x_{n+1} = x_n + h$, and $x_{N+1} = 1$. For this uniform mesh, the elements $\Omega_n = [x_n, x_{n+1}), n = 1, \ldots, N$, are of equal length h. Introduce a linear map from the nth element $x \in \Omega_n$ to the parent segment $\xi \in [-1, 1)$,

$$\xi|_{\Omega_n}(x) = \frac{2}{h}(x - x_n) - 1, \quad x \in \Omega_n. \tag{3.1}$$

For an FR scheme of order P, let $\boldsymbol{x}_n = (x_{n,p})_{p=1,2,\ldots,P+1}$ denote the set of solution points Ω_n^δ in the nth element, which map to $\boldsymbol{\xi} = (\xi_p)_{p=1,2,\ldots,P+1}$ in the parent space. The numerical approximation, $f^\delta(x)$, when restricted to Ω_n, is defined as the interpolant to the actual function $f(x)$ through $\boldsymbol{x}_n$. For instance, from (2.24), we are interested in evaluating the numerical derivative of the Fourier component, $f(x) = \exp(ikx)$. In this case,

$$f^\delta(x) = (\mathcal{P}f)(x) = \sum_{p=1}^{P+1} \exp(ikx_{n,p})\ell_p(\xi(x)), \quad x \in \Omega_n, \tag{3.2}$$

where ℓ_p is the pth Lagrange polynomial in the parent segment. The numerical approximation can equivalently be represented in vector notation as

$$\begin{aligned} \boldsymbol{f}_n^{\boldsymbol{\delta}} &:= f^\delta(x_{n,p})_{p=1,2,\ldots,P+1} \\ &= \exp(ikx_n)\left(\exp\left(ik\frac{h}{2}(1+\xi_p)\right)\right)_{p=1,2,\ldots,P+1}. \end{aligned} \tag{3.3}$$

The numerical derivative, $\frac{d^\delta f}{dx^\delta}(x \in \Omega_n)$, is obtained by differentiating f^δ after it has been " corrected" to ensure continuity across the two ends of the element. Towards this end, common interface values are first computed using the polynomial functions on either side of the interface,

$$f_I^\delta(x_n) = (1-\alpha)f^\delta(x_n^-) + \alpha f^\delta(x_n^+), \tag{3.4}$$

where $\alpha \in \left[0, \frac{1}{2}\right]$ denotes the upwinding coefficient since the advection wavespeed $a \geq 0$. $(\cdot)^-$, $(\cdot)^+$ denote the left- and right-hand limits, respectively. Next, the interface information is conveyed to the interior of the element through the use of

correction polynomials, $g_L(\xi)$, $g_R(\xi)$, of degree $P+1$ which satisfy the constraints

$$g_L(-1) = g_R(+1) = 1, \tag{3.5}$$

$$g_L(+1) = g_R(-1) = 0, \tag{3.6}$$

leading to the construction of the corrected approximation, $f^{\delta,c}$, a piecewise polynomial of degree $P+1$, which is globally continuous,

$$\begin{aligned} f^{\delta,c}(x) = f^{\delta}(x) &+ (f_I^{\delta}(x_n) - f^{\delta}(x_n^+))g_L(\xi(x)) \\ &+ (f_I^{\delta}(x_{n+1}) - f^{\delta}(x_{n+1}^-))g_R(\xi(x)), \quad x \in \Omega_n. \end{aligned} \tag{3.7}$$

Plugging (3.2) and (3.4) into (3.7) and taking derivatives, we get that the vector of derivative values in the nth element can be expressed compactly [6] as

$$\left(\frac{\partial^{\delta}}{\partial x}\exp(ikx)\right)(\boldsymbol{x}_n) = \left(\frac{\partial f^{\delta,c}}{\partial x}\right)(\boldsymbol{x}_n) = \frac{2}{h}\exp(ikx_n)\boldsymbol{Q}(kh;g,\alpha)\boldsymbol{f_n^{\delta}}, \tag{3.8}$$

where $\boldsymbol{f_n^{\delta}}$ is defined in (3.3) and $\boldsymbol{Q} \in \mathbb{C}^{(P+1)\times(P+1)}$ is the numerical differentiation operator in the parent space,

$$\boldsymbol{Q}(kh;g,\alpha) = \boldsymbol{D} + (1-\alpha)\boldsymbol{g_{L,\xi}}(\exp(-ikh)\boldsymbol{\ell}_+^T - \boldsymbol{\ell}_-^T) + \alpha\boldsymbol{g_{R,\xi}}(\exp(ikh)\boldsymbol{\ell}_-^T - \boldsymbol{\ell}_+^T). \tag{3.9}$$

Here $\boldsymbol{D} \in \mathbb{R}^{(P+1)\times(P+1)}$ is the polynomial differentiation operator such that

$$D_{p,m} = \frac{\mathrm{d}\ell_m}{\mathrm{d}\xi}(\xi_p), \quad p,m = 1,2,\ldots,P+1, \tag{3.10}$$

$\boldsymbol{g_{L,\xi}}, \boldsymbol{g_{R,\xi}} \in \mathbb{R}^{(P+1)\times 1}$ are the derivatives of the left-boundary and right-boundary correction functions at the solution points, and $\boldsymbol{\ell}_-, \boldsymbol{\ell}_+ \in \mathbb{R}^{(P+1)\times 1}$ are the extrapolated values of the $P+1$ Lagrange basis polynomials,

$$\ell_{+_p} = \ell_p(+1), \;\; \ell_{-_p} = \ell_p(-1), \quad p = 1,2,\ldots,P+1. \tag{3.11}$$

The second order directional derivative along x is recursively defined as the derivative of the first order derivative after it has been corrected to ensure continuity in derivative across the two ends of the element. Hence,

$$\left(\frac{\partial^{\delta}}{\partial x}\frac{\partial^{\delta}}{\partial x}\exp(ikx)\right)(\boldsymbol{x}_n) = \frac{4}{h^2}\exp(ikx_n)\boldsymbol{Q}(kh;g^{(2)},\alpha^{(2)})\boldsymbol{Q}(kh;g^{(1)},\alpha^{(1)})\boldsymbol{f_n^{\delta}}, \tag{3.12}$$

where $g^{(1)}, g^{(2)}$ denote the correction functions and $\alpha^{(1)}$, $\alpha^{(2)}$ denote the upwinding coefficients for evaluating the interface fluxes when correcting the polynomial approximation and the numerical first derivative, respectively.

3.2. Error in the first derivative operator. In this subsection, we derive the rate at which the numerical first derivative of the Fourier component, $\exp(ikx)$, converges to the exact derivative, $ik\,\exp(ikx)$, with refinement in grid spacing h. We begin by writing the pointwise error in the derivative at the vector of solution points. Using (3.3) and (3.8), pointwise error in the nth element is given by

$$\begin{aligned} \left[\left(\frac{\partial^{\delta}}{\partial x} - ik\right)\exp(ikx)\right](\boldsymbol{x}_n) &= \frac{2}{h}\boldsymbol{Q}(kh;g,\alpha)\exp(ik\boldsymbol{x}_n) - ik\exp(ik\boldsymbol{x}_n) \\ &= \frac{2}{h}\exp(ikx_n)\boldsymbol{E}(kh;g,\alpha), \end{aligned} \tag{3.13}$$

where $\boldsymbol{E}(kh; g, \alpha)$ represents the difference between the numerical and exact derivative values at the set of solution points in the parent space,

$$\boldsymbol{E}(kh; g, \alpha) = \left(\boldsymbol{Q}(kh; g, \alpha) - ik\frac{h}{2}\boldsymbol{I}\right) \exp\left(ik\frac{h}{2}(1+\boldsymbol{\xi})\right). \tag{3.14}$$

The rate of convergence of $\boldsymbol{E}(kh)$ with refinement in the nondimensional wavenumber kh can be obtained from (2.24) and (3.13) as

$$\begin{aligned} |\boldsymbol{E}(kh; g, \alpha)| &\preceq \left|\frac{h}{2}\exp(-ikx_n)\left[\left(\frac{\partial^\delta}{\partial x} - ik\right)\exp(ikx)\right](\boldsymbol{x}_n)\right| \\ &\preceq c(P)(kh)^{\sigma^{(1)}+1}, \end{aligned} \tag{3.15}$$

where $\preceq$ denotes a componentwise inequality and c is some scheme dependent constant. In order to proceed with an asymptotic analysis of this term, consider expanding $\boldsymbol{Q}(kh; g, \alpha)$ in its Taylor series about $kh = 0$ using (3.9),

$$\boldsymbol{Q}(kh) = \boldsymbol{Q}(0) + \boldsymbol{H}_L \sum_{m=1}^{\infty} \frac{(-ikh)^m}{m!} + \boldsymbol{H}_R \sum_{m=1}^{\infty} \frac{(ikh)^m}{m!}, \tag{3.16}$$

where the explicit parameterization with respect to g, α is suppressed for convenience of notation, and the component matrices are given by

$$\boldsymbol{Q}(0) = ((1-\alpha)\boldsymbol{g_{L,\xi}} - \alpha\boldsymbol{g_{R,\xi}})(\boldsymbol{\ell}_+^T - \boldsymbol{\ell}_-^T) + \boldsymbol{D}, \tag{3.17}$$

$$\boldsymbol{H}_L = (1-\alpha)\boldsymbol{g_{L,\xi}}\boldsymbol{\ell}_+^T, \tag{3.18}$$

$$\boldsymbol{H}_R = \alpha\boldsymbol{g_{R,\xi}}\boldsymbol{\ell}_-^T. \tag{3.19}$$

Similarly, expand the Fourier component in a power series about $kh = 0$,

$$\exp\left(ik\frac{h}{2}(1+\boldsymbol{\xi})\right) = \sum_{r=0}^{\infty} \frac{(ikh)^r}{r!}\boldsymbol{s}^r, \tag{3.20}$$

where $\boldsymbol{s}^r$ is the sampling of the rth degree polynomial,

$$s^r(\xi) = \left(\frac{1+\xi}{2}\right)^r, \tag{3.21}$$

on the set of solution points, $\boldsymbol{s}^r = (s^r)(\xi_p)_{p=1,2,\ldots,P+1}$. Plugging (3.17)–(3.19) and (3.20) into (3.14), the derivative error in the parent space can be written as

$$\begin{aligned} \boldsymbol{E}(kh) &= \left(\boldsymbol{Q}(0) + \boldsymbol{H}_L \sum_{m=1}^{\infty} \frac{(-ikh)^m}{m!} + \boldsymbol{H}_R \sum_{m=1}^{\infty} \frac{(ikh)^m}{m!} - ik\frac{h}{2}\boldsymbol{I}\right) \sum_{r=0}^{\infty} \frac{(ikh)^r}{r!}\boldsymbol{s}^r \\ &= \boldsymbol{Q}(0)\boldsymbol{1} + \sum_{j=1}^{\infty} (ikh)^j \boldsymbol{v}_j, \end{aligned} \tag{3.22}$$

where for $j \geq 1$,

$$\boldsymbol{v}_j = \boldsymbol{Q}(0)\frac{1}{j!}\boldsymbol{s}^j - \frac{1}{2(j-1)!}\boldsymbol{s}^{j-1} + \sum_{m=1}^{j} \frac{1}{m!(j-m)!}\left((-1)^m\boldsymbol{H}_L + \boldsymbol{H}_R\right)\boldsymbol{s}^{j-m}. \tag{3.23}$$

In order to evaluate the component terms, $\boldsymbol{v}_j$, we recognize that the matrix operators $\boldsymbol{Q}(0), \boldsymbol{H}_L, \boldsymbol{H}_R$ in (3.17)–(3.19) are dependent on primitive operators, $\boldsymbol{l}_+^T, \boldsymbol{l}_-^T, \boldsymbol{D}$, (3.10), (3.11), which are intrinsically related to polynomial interpolation. We can now enlist the action of aforementioned primitive operators on the sampled polynomial defined in (3.21),

$$\boldsymbol{l}_+^T \boldsymbol{s}^j = \begin{cases} 1, & j \le P, \\ (\mathcal{P}s^j)(\xi = 1), & j > P, \end{cases} \tag{3.24}$$

$$\boldsymbol{l}_-^T \boldsymbol{s}^j = \begin{cases} \mathrm{I}_{\{j=0\}}, & j \le P, \\ (\mathcal{P}s^j)(\xi = -1), & j > P, \end{cases} \tag{3.25}$$

$$\boldsymbol{D}\boldsymbol{s}^j = \begin{cases} \frac{j}{2}\boldsymbol{s}^{j-1}, & j \le P, \\ \frac{d(\mathcal{P}s^j)}{d\xi}(\boldsymbol{\xi}), & j > P, \end{cases} \tag{3.26}$$

where I denotes the indicator function and $\mathcal{P}$ is the collocation projection operator, (3.2). These relations follow from the observation that $s^j(\xi)$ is a polynomial of degree j and for $j \le P$ resides within $\mathbb{P}_P$ which is the space of the numerical solution.

In the results that follow, we derive the rate of convergence mentioned in (3.15) to determine the dependence of $\sigma^{(1)}$ on the polynomial order P, the upwinding coefficient α, and the correction function $g_L(\xi)$. The proofs of these results have been deferred to Appendix A to enhance readability.

LEMMA 3.1. *For any FR scheme of polynomial order P, i.e., for all choices of correction function and upwinding coefficient, $\boldsymbol{E}(kh)$ defined in* (3.14) *vanishes at an order higher than or equal to $P+1$,*

$$\boldsymbol{E}(kh) = \sum_{j=P+1}^{\infty} (ikh)^j \boldsymbol{v}_j, \tag{3.27}$$

where $\boldsymbol{v}_j$ is as defined in (3.23).

Lemma 3.1 and (3.15) show that for any convergent FR scheme of order P, $\sigma^{(1)} \ge P$. In order to investigate the possibility of superconvergence, we need to simplify terms in (3.23) for $j > P$. As polynomials of degree $j > P$ cannot be interpolated exactly using only $P+1$ points, we require a couple of preliminary results adapted from error estimates in Lagrange interpolation.

LEMMA 3.2. *Given a set of $P+1$ distinct points, ξ_p for $p = 1, 2, \ldots, P+1$, arranged symmetrically in $[-1, 1]$ and the collocation projection operator $\mathcal{P}$,* (3.2), *we have the following identities:*

1. $(\mathcal{P}s^{P+1})(\xi = 1) - (\mathcal{P}s^{P+1})(\xi = -1) = 1 + \frac{1}{2^{P+1}}\left((-1)^{P+1} - 1\right) \prod_{q=1}^{P+1} (1 - \xi_q)$.
2. $\frac{d(\mathcal{P}s^{P+1})}{d\xi}(\xi_p) = \frac{P+1}{2}\left(\frac{1+\xi_p}{2}\right)^P - \frac{1}{2^{P+1}} \prod_{\substack{q=1 \\ q \ne p}}^{P+1} (\xi_p - \xi_q)$.

Lemma 3.2 explores the effect of extrapolation and differentiation operators on a polynomial that is one degree higher than the dimension of the polynomial basis. This allows us to simplify $\boldsymbol{v}_{P+1}$ in this next result.

LEMMA 3.3. *For a given FR scheme of order P, if the solution points $\boldsymbol{\xi}$ are distinct and distributed symmetrically, then, in the limit $kh \to 0$, $\boldsymbol{E}(kh; g, \alpha)$ vanishes at an order*

- $\leq P+1$ *for odd* P,
- $\geq P+2$ *for even* P *if and only if*

$$(1-\alpha)g_{L,\xi_p} - \alpha g_{R,\xi_p} = -\frac{1}{2}\frac{\prod_{\substack{q=1\\ q\neq p}}^{P+1}(\xi_p-\xi_q)}{\prod_{q=1}^{P+1}(1-\xi_q)}, \quad p=1,2,\ldots,P+1, \tag{3.28}$$

where $g_{L,\xi_p} = \frac{dg_L}{d\xi}(\xi_p)$ *and* $g_{R,\xi_p} = \frac{dg_R}{d\xi}(\xi_p)$, *respectively.*

Lemma 3.3 establishes an upper bound on the rate of convergence of the derivative for odd P. Coupled with the result from Lemma 3.1 it implies that $\sigma^{(1)} = P$ if P is odd. At the same time, it shows that if P is even, then under special circumstances the rate of convergence can be higher, i.e., $\sigma^{(1)} \geq P+1$. An upper bound for even P can be derived by simplifying the term $\boldsymbol{v}_{P+2}$. This is illustrated next for the special case of $P=0$.

LEMMA 3.4. *For the FR scheme of order* $P=0$, *in the limit* $kh \to 0$, $\boldsymbol{E}(kh;\alpha)$ *vanishes at the rate*

- $(kh)^2$ *if* $\alpha \neq \frac{1}{2}$,
- $(kh)^3$ *if* $\alpha = \frac{1}{2}$.

Lemma 3.4 shows that the simple finite volume scheme enjoys an enhanced rate of convergence. For $\alpha \neq \frac{1}{2}$, $\sigma^{(1)}=1$, and for $\alpha=\frac{1}{2}$, $\sigma^{(1)}=2$. However, such additional superconvergence is not retained for any other even P. We are now ready to state the final result of this subsection.

THEOREM 3.5. *For an FR scheme of order* P, *having a symmetric set of distinct solution points* $\boldsymbol{\xi} \in [-1,1]^{P+1}$, *and symmetric correction functions* $g_{R,\xi}(\xi) = -g_{L,\xi}(-\xi)$, *the numerical first derivative converges to the exact first derivative at the order* $\sigma^{(1)}$,

$$\lim_{h\to 0}\left|\left(\frac{\partial^\delta}{\partial x} - ik\right)\exp(ikx)\right| \leq c_1\, k^{\sigma^{(1)}+1}\, h^{\sigma^{(1)}}, \quad x\in\Omega^\delta, \tag{3.29}$$

where h *denotes the element width,* $c_1(P,g,\alpha)$ *is a scheme dependent constant,* Ω^δ *is the set of solution points and*

1. $\sigma^{(1)} = \begin{cases} 1, & \alpha \neq \frac{1}{2}, \\ 2, & \alpha = \frac{1}{2} \end{cases}$ *for* $P=0$,
2. $\sigma^{(1)} = P$ *for odd* P,
3. $\sigma^{(1)} \geq P+1$ *for even* P *provided, for* $p=1,2,\ldots,P+1$,

$$\begin{cases} g_{L,\xi_p} = g_{L,\xi_{P+2-p}} = -\frac{1}{2}\dfrac{\prod_{\substack{q=1\\ q\neq p}}^{P+1}(\xi_p-\xi_q)}{\prod_{q=1}^{P+1}(1-\xi_q)}, & \alpha \neq \frac{1}{2}, \\ g_{L,\xi_p} + g_{L,\xi_{P+2-p}} = -\dfrac{\prod_{\substack{q=1\\ q\neq p}}^{P+1}(\xi_p-\xi_q)}{\prod_{q=1}^{P+1}(1-\xi_q)}, & \alpha = \frac{1}{2}, \end{cases} \tag{3.30}$$

where $g_{L,\xi_p} = \frac{dg_L}{d\xi}(\xi_p)$, *or* $\sigma^{(1)} = P$ *otherwise.*

3.3. Error in the second derivative operator. The second derivative in FR is defined recursively as the derivative of the corrected first derivative which itself is the derivative of the corrected polynomial approximation. The procedure involves two corrections, one for the polynomial approximation, with correction function $g_L^{(1)}$ and upwinding coefficient $\alpha^{(1)}$, and one for the first derivative, with correction function $g_L^{(2)}$ and upwinding coefficient $\alpha^{(2)}$. Using (3.12), the pointwise error in evaluation of the second derivative at the vector of solution points is given by

$$\begin{aligned}
&\left[\left(\frac{\partial^\delta}{\partial x}\frac{\partial^\delta}{\partial x}+k^2\right)\exp(ikx)\right](\boldsymbol{x}_n)\\
&=\frac{4}{h^2}\boldsymbol{Q}(kh;g^{(2)},\alpha^{(2)})\boldsymbol{Q}(kh;g^{(1)},\alpha^{(1)})\exp(ik\boldsymbol{x}_n)+k^2\exp(ik\boldsymbol{x}_n)\\
&=\frac{4}{h^2}\exp(ikx_n)\boldsymbol{F}(kh;g^{(2)},g^{(1)},\alpha^{(2)},\alpha^{(1)}),
\end{aligned}\tag{3.31}$$

where $\boldsymbol{F}$ represents the difference between the numerical and exact second derivative values at the set of solution points in the parent space,

$$\begin{aligned}
&\boldsymbol{F}(kh;g^{(2)},g^{(1)},\alpha^{(2)},\alpha^{(1)})\\
&=\left[\boldsymbol{Q}(kh;g^{(2)},\alpha^{(2)})\boldsymbol{Q}(kh;g^{(1)},\alpha^{(1)})+\frac{h^2k^2}{4}\right]\exp\left(ik\frac{h}{2}(1+\boldsymbol{\xi})\right).
\end{aligned}\tag{3.32}$$

Once again, from (2.25) and (3.31), it follows that

$$|\boldsymbol{F}(kh;g^{(2)},g^{(1)},\alpha^{(2)},\alpha^{(1)})|\preceq c(P)(kh)^{\sigma^{(2)}+2}\tag{3.33}$$

for some scheme dependent constant c. As in the previous subsection, an asymptotic analysis of this term can be performed through a power series expansion in kh about 0. However, the algebraic accounting becomes exceptionally tedious. Nevertheless, a lower bound on the rate of convergence can be readily achieved by substituting (3.14) into (3.32). Denoting $\boldsymbol{Q}(kh;g^{(m)},\alpha^{(m)})$ as $\boldsymbol{Q}^{(m)}$ for $m=1,2$ and suppressing parameterization where apparent, we get that

$$\begin{aligned}
\boldsymbol{F}&=\boldsymbol{Q}^{(2)}\left(\boldsymbol{Q}^{(1)}\exp\left(ik\frac{h}{2}(1+\boldsymbol{\xi})\right)\right)+\frac{h^2k^2}{4}\exp\left(ik\frac{h}{2}(1+\boldsymbol{\xi})\right)\\
&=\boldsymbol{Q}^{(2)}\left(\boldsymbol{E}(kh;g^{(1)},\alpha^{(1)})+ik\frac{h}{2}\exp\left(ik\frac{h}{2}(1+\boldsymbol{\xi})\right)\right)+\frac{h^2k^2}{4}\exp\left(ik\frac{h}{2}(1+\boldsymbol{\xi})\right)\\
&=\boldsymbol{Q}^{(2)}\boldsymbol{E}(kh;g^{(1)},\alpha^{(1)})+ik\frac{h}{2}\left(\boldsymbol{E}(kh;g^{(2)},\alpha^{(2)})+ik\frac{h}{2}\exp\left(ik\frac{h}{2}(1+\boldsymbol{\xi})\right)\right)\\
&\qquad+\frac{h^2k^2}{4}\exp\left(ik\frac{h}{2}(1+\boldsymbol{\xi})\right)\\
&=\boldsymbol{Q}^{(2)}\boldsymbol{E}(kh;g^{(1)},\alpha^{(1)})+ik\frac{h}{2}\boldsymbol{E}(kh;g^{(2)},\alpha^{(2)}),
\end{aligned}\tag{3.34}$$

which shows that error in the second derivative operator can be determined from the error in the two constituent first derivative operators. As a specific example, consider the case of $P=0$ for which the following result can be established.

LEMMA 3.6. *For an FR scheme of order $P=0$, in the limit $kh\to 0$, $\boldsymbol{F}(kh)$ vanishes at the rates*

- $(kh)^3$ *if* $\alpha^{(1)} + \alpha^{(2)} \neq 1$,
- $(kh)^4$ *if* $\alpha^{(1)} + \alpha^{(2)} = 1$.

Lemma 3.6 highlights the importance of having an isotropic operator. In order to derive an asymptotic bound for $P > 0$, let $\sigma^{(1),1}$ and $\sigma^{(1),2}$ be the rates of convergence associated with the two first derivative operators involved. From (3.15) and (3.22), this can be expressed as

$$\boldsymbol{E}(kh; g^{(m)}, \alpha^{(m)}) = \sum_{j=\sigma^{(1),m}+1}^{\infty} (ikh)^j \boldsymbol{v}_j^{(m)}, \quad m = 1, 2. \tag{3.35}$$

We can now state the following result regarding a lower bound for the rate of convergence of the second derivative.

THEOREM 3.7. *For an FR scheme having a symmetric set of distinct solution points and symmetric correction functions, the numerical second derivative converges to the exact second derivative at the order* $\sigma^{(2)}$,

$$\lim_{h\to 0} \left| \left(\frac{\partial^\delta}{\partial x} \frac{\partial^\delta}{\partial x} + k^2 \right) \exp(ikx) \right| \leq c_2 \, k^{\sigma^{(2)}+2} \, h^{\sigma^{(2)}}, \quad x \in \Omega^\delta, \tag{3.36}$$

where h *denotes the element width,* $c_2(P, g^{(2)}, g^{(1)}, \alpha^{(2)}, \alpha^{(1)})$ *is a scheme dependent constant,* Ω^δ *is the set of solution points, and*

1. $\sigma^{(2)} = \begin{cases} 1, & \alpha^{(1)} + \alpha^{(2)} \neq 1, \\ 2, & \alpha^{(1)} + \alpha^{(2)} = 1 \end{cases}$ *for* $P = 0$,
2. $\sigma^{(2)} \geq \min\left(\sigma^{(1),1} - 1, \sigma^{(1),2}\right)$ *for* $P > 0$,

where $\sigma^{(1),1}, \sigma^{(1),2}$ *are the rates of convergence of the two first derivative operators involved in differentiating the polynomial approximation and the first derivative, respectively.*

Theorems 3.5 and 4.3 combined with (2.26) yield the following lower bound.

COROLLARY 3.8. *The order of convergence of error in the* $\mathcal{L}^\delta(\Omega^\delta)$ *seminorm,* (2.23)*, is given by* σ,

$$\begin{aligned} \lim_{h\to 0} \|e_u\|_{\mathcal{L}^\delta(\Omega^\delta)} &\leq C' \left[|a| \, k^{\sigma^{(1)}+1} \, h^{\sigma^{(1)}} + b \, k^{\sigma^{(2)}+2} \, h^{\sigma^{(2)}} \right] \\ &\leq C \, h^\sigma, \end{aligned} \tag{3.37}$$

where $C(P, g^{(2)}, g^{(1)}, \alpha^{(2)}, \alpha^{(1)}, a, b, k)$ *is a scheme, equation dependent constant, and*

$$\sigma \geq \min(\sigma^{(1)}, \sigma^{(2)}) \geq P - 1, \tag{3.38}$$

where $\sigma^{(1)}$, $\sigma^{(2)}$ *are the rates of convergence of respective derivative operators as described in Theorems* 3.5 *and* 3.7.

3.4. Superconvergent FR (SFR) schemes. Theorem 3.5 shows that the rate of convergence of the numerical first derivative operator depends on whether P is odd or even. For odd P, the order is exactly P irrespective of the choice of correction function or upwinding coefficient. However, for even P, superconvergence can be achieved under special conditions. In particular, for such superconvergence, (i) the correction function is identified uniquely if the interface flux is not centered, and (ii) a family of correction functions exists if the interface flux is centered. This family

is parameterized by $P/2$ free parameters. One possible choice for the parameter set is the correction function derivatives, $g_{L,\xi_p} = \frac{dg_L}{d\xi}(\xi_p)$, at the solution points in the left half of the parent space, i.e., $p = 1, 2, \ldots, \frac{P}{2}$. The remaining derivatives are then prescribed by (3.30) as

$$g_{L,\xi_{P+2-p}} = -g_{L,\xi_p} - \frac{\prod_{\substack{q=1 \\ q\neq p}}^{P+1} (\xi_p - \xi_q)}{\prod_{q=1}^{P+1} (1 - \xi_q)}, \quad p = 1, 2, \ldots, \frac{P}{2}, \tag{3.39}$$

$$g_{L,\xi_{\frac{P}{2}+1}} = -\frac{1}{2} \frac{\prod_{\substack{q=1 \\ q\neq p}}^{P+1} (\xi_p - \xi_q)}{\prod_{q=1}^{P+1} (1 - \xi_q)}. \tag{3.40}$$

We designate this family as superconvergent flux reconstruction (SFR). The specification in (3.39)–(3.40) ensures that the first derivative operator is superconvergent. However, the stability of the corresponding SFR scheme is not guaranteed. From a practical point of view, the scheme should be stable, at least in the von Neumann sense, for pure advection. We can test linear stability/instability by computing eigenvalues of the resulting operator matrix, (3.9). The condition for numerical stability [16, 6] is given by

$$\lambda_p^{\mathrm{Im}}(kh) \leq 0 \text{ for } p = 1, 2, \ldots, P+1, \quad k \in \left[0, \frac{(P+1)\pi}{h}\right], \tag{3.41}$$

where $\frac{ikh}{2}\lambda_p$ is the pth eigenvalue of $\boldsymbol{Q}$. In the case of $\alpha \neq \frac{1}{2}$, the unique superconvergent scheme identified in Theorem 3.5 is, in fact, unstable at least for $P = 2$ and $P = 4$. However, for $\alpha = \frac{1}{2}$, a family of linearly stable schemes exists. Figure 1(a) plots $\max_p \lambda_p^{\mathrm{Im}}(kh)$ for $P = 2$ against the free parameter g_{L,ξ_1}. We see that all schemes for which $g_{L,\xi_1} < -2.524$ are stable. Figure 1(b) plots the region of stability for this family for $P = 4$. We see that the scheme is stable when g_{L,ξ_1}, g_{L,ξ_2} is chosen from within a convex subset of $\mathbb{R}^2$. A vertex of this region is located at $g_{L,\xi_1} = -5.906, g_{L,\xi_2} = 1.422$.

Figure 2(a) plots the correction function g_L for $\xi \in [-1, 1]$ for four stable members of the SFR family, viz. the boundary scheme with $g_{L,\xi_1} = -2.524$, the collocation-based nodal discontinuous Galerkin (DG) scheme with centered interface fluxes, and the schemes with g_{L,ξ_1} as $-3.0, -4.0$, respectively. We see that as the parameter g_{L,ξ_1} decreases, the first root of the correction function moves to the left while the second moves to the right. A similar plot for $P = 4$ is recorded in Figure 2(b) for the four schemes marked in Figure 1(b) and recorded in Table 2.

Interestingly, the nodal DG scheme with centered fluxes is recovered as one member of this family, while the FR version of the spectral difference (SD) scheme [16] is not. For both $P = 2$ and $P = 4$, the DG scheme lies close to the stability boundary. This space of linearly stable schemes can be utilized as the feasible set for an optimization problem to maximize accuracy [5]. Preliminary results suggest that the optimal solution set may not contain the DG scheme. However, we will defer a thorough investigation into such optimal schemes to a future investigation.

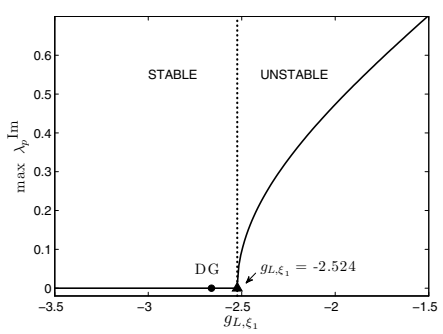

(a) $P = 2$: Maximum imaginary eigenvalue against the free parameter g_{L,ξ_1}.

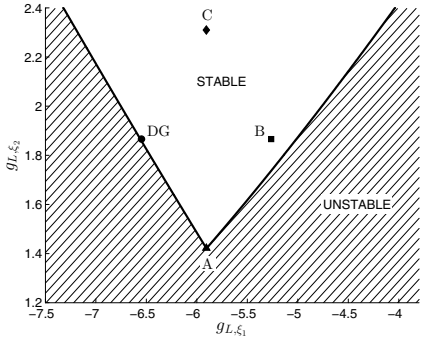

(b) $P = 4$: Region of stability in the space of the two parameters $(g_{L,\xi_1}, g_{L,\xi_2})$.

FIG. 1. *Region of stability in the parameter space,* (3.39)*, for the superconvergent family of schemes, SFR, defined in section* 3.4.

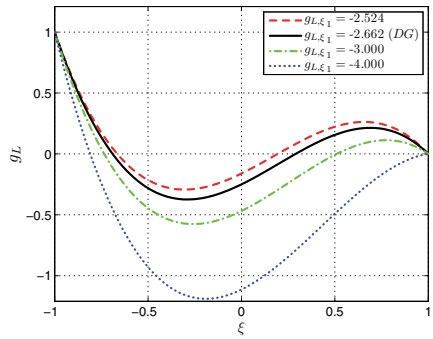

(a) P=2

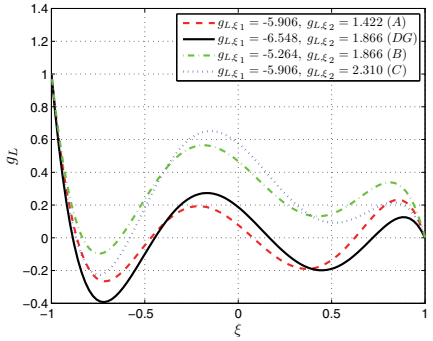

(b) P=4

FIG. 2. *Left-boundary correction function for the superconvergent family of schemes defined in section* 3.4.

TABLE 2
$P = 4$: Parameters for the SFR schemes marked in Figure 1(b).

Scheme	g_{L,ξ_1}	g_{L,ξ_2}
A	−5.9060	1.4220
DG	−6.5480	1.8661
B	−5.2640	1.8661
C	−5.9060	2.3102

4. Rates of convergence via eigensolution analysis. Corollary 3.8 provides an estimate for the rate of convergence of error in the $\mathcal{L}^\delta(\Omega^\delta)$ seminorm. In order to obtain estimates in the $\ell^2(\Omega^\delta)$ norm, we now introduce the eigensolution to the steady-state error equation, (2.19)–(2.20). This allows us to express the pointwise error, (2.18), in terms of the eigenvalues and eigenvectors associated with the numerical differentiation operator $\boldsymbol{Q}$. By utilizing results derived in [6], this section derives the

rate of convergence for the steady-state numerical solution as well as the first and second order derivative operators. As in section 3, the proofs of results have been deferred to Appendix B to enhance readability.

4.1. Eigensolution convergence estimate for the first derivative operator. Recognizing that the derivative operator $\boldsymbol{Q}(kh; g, \alpha)$, (3.9), is linear, we can decouple the derivative values at the $P+1$ solution points by a change of basis,

$$\boldsymbol{Q}(kh) = \boldsymbol{W}(kh) ik\frac{h}{2}\boldsymbol{\Lambda}(kh)\boldsymbol{W}^{-1}(kh), \tag{4.1}$$

where $\boldsymbol{\Lambda}$ is the diagonal matrix of normalized eigenvalues, $\lambda_p(kh) \in \mathbb{C}, p = 1, \ldots, P+1$, and $\boldsymbol{W} \in \mathbb{C}^{P+1\times P+1}$ is the dense matrix containing eigenvectors of the differentiation operator. The explicit parameterization with respect to g and α has again been suppressed for ease of notation. Assuming that the differentiation operator is indeed diagonalizable, the sampled Fourier component, (3.3), can be expanded in the basis of the eigenvectors,

$$\exp\left(ik\frac{h}{2}(1+\boldsymbol{\xi})\right) = \boldsymbol{W}(kh)\boldsymbol{\beta}(kh), \tag{4.2}$$

where $\beta_p(kh) \in \mathbb{C}$ is the expansion coefficient along the pth column of $\boldsymbol{W}$, $\boldsymbol{w}_p(kh)$, for $p = 1, 2, \ldots, P+1$. The derivative error in the parent space, (3.14), can now be written as

$$\begin{aligned}\boldsymbol{E}(kh) &= \left(\boldsymbol{W}(kh) ik\frac{h}{2}\boldsymbol{\Lambda}(kh)\boldsymbol{W}^{-1}(kh) - ik\frac{h}{2}\boldsymbol{I}\right)\boldsymbol{W}(kh)\boldsymbol{\beta}(kh)\\ &= ik\frac{h}{2}\boldsymbol{W}(kh)\left(\boldsymbol{\Lambda}(kh) - \boldsymbol{I}\right)\boldsymbol{\beta}(kh)\\ &= ik\frac{h}{2}\sum_{p=1}^{P+1}\left(\lambda_p(kh) - 1\right)\beta_p(kh)\boldsymbol{w}_p(kh),\end{aligned} \tag{4.3}$$

which shows that the error in the first derivative operator is a sum of the errors in the eigenvalues, $\lambda_p(kh) - 1$, weighted by the modal weights β_p for the $P+1$ modes.

Lemmas 3.4, 3.5, and 3.6 of [6] show that, for any FR scheme, a unique "physical" mode exists for which the normalized eigenvalue $\lambda_1(kh) \to 1$ and the modal weight $\beta_1(kh) \to \sqrt{P+1}$ as $kh \to 0$. All other modes are spurious such that their modal weights vanish $\beta_p(kh) \to 0$, $p = 2, \ldots, P+1$ in the asymptotic limit. Correspondingly, we can define the rate of convergence of the normalized physical eigenvalue, $q_1^\lambda > 0$,

$$|\lambda_1(kh) - 1| \le c_1^\lambda\,(kh)^{q_1^\lambda} \quad \text{as } kh \to 0 \tag{4.4}$$

for some constant c_1^λ. Similarly, we can define the rates of convergence of modal weights, $q_p^\beta > 0$,

$$\left|\beta_p(kh) - \sqrt{P+1}\delta_{1p}\right| \le c_p^\beta\,(kh)^{q_p^\beta}, \quad p = 1, \ldots, P+1 \ \text{ as } kh \to 0 \tag{4.5}$$

for some constants c_p^β, $p = 1, \ldots, P+1$. Here $\delta_{1p} = \mathrm{I}_{\{p=1\}}$. These definitions provide the first result of this section.

LEMMA 4.1. *For an FR scheme of order P, the numerical first derivative converges to the exact first derivative, at the set of solution points, at the order $\sigma^{(1)}$, defined in* (3.29)*, where*

$$\sigma^{(1)} \geq \min_{p=2}^{P+1} \left(q_1^{\lambda}, q_p^{\beta}, q_p^{\lambda\beta}\right), \tag{4.6}$$

and q_1^{λ}, q_p^{β} are as defined in (4.4), (4.5)*, and $q_p^{\lambda\beta} > 0$ for $p = 2, \ldots, P+1$ are the asymptotic rates of convergence of the product of eigenvalues and modal weights,*

$$|\lambda_p(kh)\beta_p(kh)| \leq c_p^{\lambda\beta}(kh)^{q_p^{\lambda\beta}}, \quad p = 2, \ldots, P+1 \ \text{ as } kh \to 0. \tag{4.7}$$

4.2. Eigensolution convergence estimate for the second derivative operator. An eigensystem approach for analyzing the error in the second derivative is complicated by the possibility of different operators in the two corrections. However, in the special case that both corrections are performed using the same g and α, i.e.,

$$\boldsymbol{Q}(kh; g^{(2)}, \alpha^{(2)}) = \boldsymbol{Q}(kh; g^{(1)}, \alpha^{(1)}) = \boldsymbol{Q}(kh; g, \alpha), \tag{4.8}$$

the rate of convergence can be derived in a manner analogous to the previous subsection. Error in the parent space, (3.32), can then be written as

$$\begin{aligned}
\boldsymbol{F}(kh) &= \left[\boldsymbol{W}(kh)\left(ik\frac{h}{2}\right)^2 \boldsymbol{\Lambda}^2(kh)\boldsymbol{W}^{-1}(kh) + \frac{h^2k^2}{4}\boldsymbol{I}\right]\boldsymbol{W}(kh)\boldsymbol{\beta}(kh) \\
&= -\frac{k^2h^2}{4}\boldsymbol{W}(kh)\left[\boldsymbol{\Lambda}^2(kh) - \boldsymbol{I}\right]\boldsymbol{\beta}(kh) \\
&= -\frac{k^2h^2}{4}\sum_{p=1}^{P+1}\left(\lambda_p^2(kh) - 1\right)\beta_p(kh)\boldsymbol{w}_p(kh). \qquad (4.9)
\end{aligned}$$

This provides us with the next result of this section.

LEMMA 4.2. *For an FR scheme of order P that uses the same correction function and upwinding coefficient for the two corrections, the numerical second derivative converges to the exact second derivative, at the set of solution points, at the order $\sigma^{(2)}$, defined in* (3.36)*, where*

$$\sigma^{(2)} \geq \min_{p=2}^{P+1} \left(q_1^{\lambda}, q_p^{\beta}, 2q_p^{\lambda\beta} - q_p^{\beta}\right), \tag{4.10}$$

and $q_1^{\lambda}, q_p^{\beta}$, and $q_p^{\lambda\beta}$ are defined in (4.4), (4.5)*, and* (4.7)*, respectively.*

As an example, the various rates of convergence involved in Lemmas 4.1 and 4.2 are recorded in Table 3 for the DG scheme for polynomial orders $P = 0$ to 5.

4.3. Eigensolution convergence estimate for the steady-state solution. We now derive the rate of convergence error in the $\ell^2(\Omega^{\delta})$ norm in terms of the asymptotic eigensystem associated with the differentiation operator $Q(kh)$. As in section 4.2, we only consider the special case when all three involved corrections use the same correction function g and upwinding coefficient α. The left-hand side of (2.19) can then be written in vector notation at the set of solution points in the nth

TABLE 3

Rates of convergence of the eigensystem components for the DG scheme using Gauss–Legendre solution points. The rates are determined directly by computing the eigensolution as a function of kh [6].

	$\alpha = 0$				$\alpha = \frac{1}{2}$			
P	q_1^λ	$\min_{p=2}^{P+1} q_p^\beta$	$\min_{p=2}^{P+1} q_p^{\lambda\beta}$	$\min_{p=2}^{P+1} 2q_p^{\lambda\beta} - q_p^\beta$	q_1^λ	$\min_{p=2}^{P+1} q_p^\beta$	$\min_{p=2}^{P+1} q_p^{\lambda\beta}$	$\min_{p=2}^{P+1} 2q_p^{\lambda\beta} - q_p^\beta$
0	1	-	-	-	2	-	-	-
1	3	2	1	0	2	1	1	1
2	5	3	2	1	6	4	3	2
3	7	4	3	2	6	3	3	2
4	9	5	4	3	10	6	5	4
5	11	6	5	4	10	5	5	4

element using (4.1) as

$$\begin{aligned}(\mathcal{L}^\delta e_u)(\boldsymbol{x_n}) &= \left(\frac{2}{h}a\boldsymbol{Q}(kh) - \frac{4}{h^2}b\boldsymbol{Q}^2(kh)\right)e_u(\boldsymbol{x}_n)\\ &= \boldsymbol{W}(kh)(iak\boldsymbol{\Lambda}(kh) + bk^2\boldsymbol{\Lambda}^2(kh))\boldsymbol{W}^{-1}(kh)e_u(\boldsymbol{x}_n)\\ &= \boldsymbol{W}(kh)\boldsymbol{\Pi}(k,h)\boldsymbol{W}^{-1}(kh)e_u(\boldsymbol{x}_n),\end{aligned} \tag{4.11}$$

where $\boldsymbol{\Pi}$ is the diagonal matrix of eigenvalues, $\pi_p(k,h) = iak\lambda(kh) + bk^2\lambda^2(kh)$, $p = 1, \ldots, P+1$, of the numerical advection-diffusion operator. Similarly, the right-hand side of (2.19) can be written in vector form using (2.21), (3.13), (3.31), (4.3), and (4.9) at the set of solution points in the nth element as

$$\begin{aligned}\left((\mathcal{L} - \mathcal{L}^\delta)\exp(ikx)\right)(\boldsymbol{x_n}) &= -a\frac{2}{h}\exp(ikx_n)\boldsymbol{E}(kh) + b\frac{4}{h^2}\exp(ikx_n)\boldsymbol{F}(kh)\\ &= -\exp(ikx_n)\boldsymbol{W}(kh)\Big[\boldsymbol{\Pi}(k,h) - (iak + bk^2)\boldsymbol{I}\Big]\boldsymbol{\beta}(kh).\end{aligned} \tag{4.12}$$

Substituting (4.11) and (4.12) into (2.19), and noting that $\pi_p(k,h) \neq 0$, we get

$$\begin{aligned}e_u(\boldsymbol{x}_n) &= -\exp(ikx_n)\boldsymbol{W}(kh)\boldsymbol{\Pi}^{-1}(k,h)\left[\boldsymbol{\Pi}(k,h) - (iak + bk^2)\boldsymbol{I}\right]\boldsymbol{\beta}(kh)\\ &= \exp(ikx_n)\sum_{p=1}^{P+1}\left((iak + bk^2)\pi_p^{-1}(k,h) - 1\right)\beta_p(kh)\boldsymbol{w}_p(kh),\end{aligned} \tag{4.13}$$

which brings us to the last result of this section.

THEOREM 4.3. *For an FR scheme of order P that uses the same correction function and upwinding coefficient for all three corrections, the order of convergence of error in the $\ell^2(\Omega^\delta)$ norm, (2.22), is given by μ,*

$$\lim_{h\to 0} \|e_u\|_{\ell^2(\Omega^\delta)} \leq C\, h^\mu, \tag{4.14}$$

where $C(k,a,b,P)$ is some scheme, equation dependent constant, and

$$\mu \geq \min_{p=2}^{P+1}\left(q_1^\lambda, q_p^\beta\right), \tag{4.15}$$

where q_1^λ and q_p^β are as defined in (4.4) and (4.5), respectively.

Theorem 4.3 shows that the rate of convergence for steady-state problems is identical to the short-time rate of convergence for unsteady problems derived in [6] and tabulated in Table 1.

5. Numerical verification. This section consists of two parts. In the first part, we verify the analytical estimates for rates of convergence of derivative operators derived in Theorems 3.5 and 3.7 and their Fourier counterparts in Lemmas 4.1 and 4.2. In the second part, we conduct a simple numerical experiment to verify the estimate for rate of convergence of error in the $\mathcal{L}^\delta(\Omega^\delta)$ seminorm, Corollary 3.8, and the $\ell^2(\Omega^\delta)$ norm, Theorem 4.3.

5.1. Rate of convergence for derivative operators. We begin by employing the first and second order FR operators to differentiate the simple sinusoid, $u(x) = \cos(2\pi x)$, in $[0, 1]$. Error is measured using the $\ell^2(\Omega^\delta)$ norm for both the first and second order derivatives. The rate of convergence is calculated numerically by using two grids with spacing $h_1 = 1/32$ and $h_2 = 1/64$ and rounded to three decimal places. The left and right correction functions are chosen to be the right and left Radau polynomials, respectively, in order to recover the DG scheme [16]. The solution points in each element are chosen to be the Gauss–Legendre points in the parent space. Rates are obtained for $P = 0$ to 5 for both one-sided and centered fluxes. For the first derivative, the upwind flux is given by $\alpha = 0$ and the centered flux by $\alpha = 1/2$. For the second derivative, the one-sided flux is given by $\alpha^{(1)} = 0$, $\alpha^{(2)} = 1$ in the isotropic case or by $\alpha^{(1)} = 0$, $\alpha^{(2)} = 0$ in the anisotropic case; the centered flux is given by $\alpha^{(1)} = \alpha^{(2)} = 1/2$.

TABLE 4
Rate of convergence for the first derivative operator, $\sigma^{(1)}$, in $\ell^2(\Omega^\delta)$ norm using DG.

	Theorem 3.5		Lemma 4.1		Grid-convergence study	
P	$\alpha = 0$	$\alpha = \frac{1}{2}$	$\alpha = 0$	$\alpha = \frac{1}{2}$	$\alpha = 0$	$\alpha = \frac{1}{2}$
0	1	2	1	2	0.999	1.998
1	1	1	1	1	0.997	0.994
2	2	3	2	3	2.004	3.004
3	3	3	3	3	2.998	2.995
4	4	5	4	5	4.002	5.000
5	5	5	5	5	4.999	4.995

TABLE 5
Rate of convergence for the second derivative operator, $\sigma^{(2)}$, in $\ell^2(\Omega^\delta)$ norm using DG. Note that Lemma 4.2 has been proven to hold only for the case of $\alpha^{(2)} = \alpha^{(1)}$.

	Theorem 3.7			Lemma 4.2			Grid-convergence study		
	$\alpha^{(1)} = 0$	$\alpha^{(1)} = 0$	$\alpha^{(1)} = \frac{1}{2}$	$\alpha^{(1)} = 0$	$\alpha^{(1)} = 0$	$\alpha^{(1)} = \frac{1}{2}$	$\alpha^{(1)} = 0$	$\alpha^{(1)} = 0$	$\alpha^{(1)} = \frac{1}{2}$
P	$\alpha^{(2)} = 0$	$\alpha^{(2)} = 1$	$\alpha^{(2)} = \frac{1}{2}$	$\alpha^{(2)} = 0$	$\alpha^{(2)} = 1$	$\alpha^{(2)} = \frac{1}{2}$	$\alpha^{(2)} = 0$	$\alpha^{(2)} = 1$	$\alpha^{(2)} = \frac{1}{2}$
0	1	2	2	1	1	2	0.997	1.999	1.994
1	0	0	0	0	0	1	−0.008	−0.003	0.988
2	1	1	2	1	1	2	1.014	1.005	2.014
3	2	2	2	2	2	2	1.996	1.998	2.041
4	3	3	4	3	3	4	3.005	3.003	4.002
5	4	4	4	4	4	4	3.997	3.998	4.010

The results are tabulated in Tables 4 and 5 for the two derivatives. For the first derivative, Table 4 shows that the numerical convergence rates are in exact agreement with the theoretical convergence rates stated in Theorem 3.5 and Lemma 4.1. In the case of the second derivative, Table 5 shows that the eigenvalue estimate, Lemma 4.2, is exact for all cases except $P = 0$ with the one-sided, isotropic flux. This is not

surprising since Lemma 4.2 strictly holds only when the same upwinding coefficient is used for the two corrections. Similarly, the bound in Theorem 3.7 is tight for all cases except for $P = 1$ with centered fluxes. A dedicated treatment of this edge case, in a manner similar to Lemma 3.6, would yield an exact match.

5.2. Rate of convergence for steady-state solution. Having established the validity of the theoretical results for derivative operators, we now return to the steady-state problem in (2.1)–(2.3) with $a = 1$, $b = 1$, $k = 4\pi$, and $k_0 = 2\pi$. We are interested in determining the rate of convergence of error in both measures, i.e., the $\mathcal{L}^\delta(\Omega^\delta)$ seminorm and the $\ell^2(\Omega^\delta)$ norm. Moreover, we are interested in determining the rate of convergence of the first and second derivative in the $\ell^2(\Omega^\delta)$ norm. Equations (2.1)–(2.3) are solved using FR in $[0, 1]$ for $P = 0$ to 5 with one-sided, isotropic ($\alpha = 0, \alpha^{(1)} = 0, \alpha^{(2)} = 1$), as well as fully centered ($\alpha = 1/2, \alpha^{(1)} = 1/2, \alpha^{(2)} = 1/2$) fluxes. Once again, Gauss–Legendre points are chosen to be the solution points and the correction functions are chosen to recover the DG scheme. The numerical solution is marched in time using a backward-Euler time stepping scheme until the equation residual falls below a tolerance of 10^{-10}. The rate of convergence is calculated using two grids with spacing $h_1 = 1/1024$ and $h_2 = 1/2048$ for $P = 0, 1$; $h_1 = 1/64$ and $h_2 = 1/128$ for $P = 2, 3$, and $h_1 = 1/16$ and $h_2 = 1/32$ for $P = 4, 5$ to avoid saturation due to finite precision.

TABLE 6

Rate of convergence of the solution, first derivative, and second derivative in $\ell^2(\Omega^\delta)$ norm for the steady, forced, advection-diffusion problem using DG.

	Theorem 4.3		Grid-convergence study					
	Solution		Solution		1st derivative		2nd derivative	
P	One-sided	Centered	One-sided	Centered	One-sided	Centered	One-sided	Centered
0	1	2	0.981	2.000	1.000	2.000	1.000	2.000
1	2	1	2.000	1.000	2.000	1.000	2.000	1.000
2	3	4	2.999	4.007	2.999	4.004	2.999	4.004
3	4	3	3.999	2.999	3.999	2.998	3.998	2.998
4	5	6	4.993	6.085	4.994	6.063	4.994	6.062
5	6	5	5.983	4.968	5.991	4.961	5.892	4.957

TABLE 7

Rate of convergence of error in $\mathcal{L}^\delta(\Omega^\delta)$ seminorm for the steady, forced, advection-diffusion problem using DG.

	Corollary 3.8		Grid convergence study	
P	One-sided	Centered	One-sided	Centered
0	1	2	0.980	2.000
1	0	0	0.000	1.000
2	1	2	1.006	2.014
3	2	2	1.996	2.041
4	3	4	3.055	4.017
5	4	4	3.959	4.092

Table 6 records the rate of convergence of the numerical solution, first derivative, and second derivative in the $\ell^2(\Omega^\delta)$ norm. Alongside, the analytical expectation from Theorem 4.3 is included for comparison. We see that theoretical expectation matches excellently with the results of the grid convergence study for all polynomial orders. In fact, even though our proof for Theorem 4.3 requires that the same upwinding coefficient be used for all three corrections, the theoretical predictions hold for both

choices of interface fluxes. Moreover, both the first and the second derivatives converge at almost exactly the same rate as the solution. This is a salient feature of FR lent by the recursive nature of the correction procedure which couples all the elements in the domain. The resulting estimates for the derivatives are therefore global and not element-local.

Table 7 records the rate of convergence of error in the $\mathcal{L}^\delta(\Omega^\delta)$ seminorm. Alongside, the analytical expectation from Corollary 3.8 is included for comparison. We see that the estimate matches excellently with the results of the grid convergence study for all polynomial orders and fluxes except for the case of $P = 1$ with centered flux. This is the same case for which the bound in Theorem 3.7 is not tight (cf. section 5.1). A dedicated treatment of this edge case, in a manner similar to Lemma 3.6, would yield an exact match.

6. Concluding remarks. The contributions of this paper can be divided into three main parts. First, in Theorems 3.5 and 3.7, we have analytically derived the rates of convergence of the numerical first and second derivative operators in FR as a function of polynomial order, correction function, and upwinding coefficients. This has resulted in the prescription of a new class of superconvergent schemes within the FR family, discussed in section 3.4. Second, in Theorem 4.3, we have shown that the rate of convergence of the vector ℓ^2 norm of error for the steady-state, forced, linear advection-diffusion problem is identical to the short-time rate of convergence for time-dependent problems derived in [6]. This highlights the importance of analyzing "spurious" modes in the eigensolution of discontinuous finite element schemes. Finally, as an empirical result, we have shown that the numerical derivatives in FR converge at the same rate as the solution, which highlights the recursive nature of the reconstruction procedure.

Appendix A. Proofs of results in section 3.

Proof of Lemma 3.1. We begin by noting that $\boldsymbol{Q}(0)\mathbf{1} = \mathbf{0}$ from Lemma 3.4 in [6]. Let $1 \leq j \leq P$ in (3.23). Then, using the properties in (3.24)–(3.26),

$$\begin{aligned}
\boldsymbol{v}_j &= \frac{1}{j!}\left((1-\alpha)\boldsymbol{g}_{\boldsymbol{L},\boldsymbol{\xi}} - \alpha\boldsymbol{g}_{\boldsymbol{R},\boldsymbol{\xi}}\right) + \frac{j}{2j!}\boldsymbol{s}^{j-1} - \frac{1}{2(j-1)!}\boldsymbol{s}^{j-1} \\
&\quad + \sum_{m=1}^{j} \frac{(-1)^m}{m!(j-m)!}(1-\alpha)\boldsymbol{g}_{\boldsymbol{L},\boldsymbol{\xi}} + \frac{1}{j!}\alpha\boldsymbol{g}_{\boldsymbol{R},\boldsymbol{\xi}} \\
&= (1-\alpha)\boldsymbol{g}_{\boldsymbol{L},\boldsymbol{\xi}}\left(\frac{1}{j!} + \sum_{m=1}^{j}\frac{(-1)^m}{m!(j-m)!}\right) \\
&= (1-\alpha)\boldsymbol{g}_{\boldsymbol{L},\boldsymbol{\xi}}\left(\frac{1}{j!} + \sum_{m=0}^{j}\frac{(-1)^m}{m!(j-m)!} - \frac{1}{j!}\right) \\
&= \mathbf{0},
\end{aligned}$$

where we have used binomial expansion so that $\sum_{m=0}^{j}\frac{(-1)^m}{m!(j-m)!} = \frac{1}{j!}(1+(-1))^j = 0$. The proof now follows from (3.22). ∎

Proof of Lemma 3.2. Let $\phi(\xi) = s^{P+1} = \left(\frac{1+\xi}{2}\right)^{P+1}$. Then from the error estimate in Lagrange interpolation, for $\xi \in [-1, 1]$,

$$\begin{aligned}\phi(\xi) - (\mathcal{P}\phi)(\xi) &= \frac{1}{(P+1)!}\frac{\partial^{P+1}\phi}{\partial\xi^{P+1}}\prod_{q=1}^{P+1}(\xi - \xi_q)\\ &= \frac{1}{2^{P+1}}\prod_{q=1}^{P+1}(\xi - \xi_q). \qquad \text{(A.1)}\end{aligned}$$

Now it is easy to see that

$$\begin{aligned}&(\mathcal{P}s^{P+1})(\xi = 1) - (\mathcal{P}s^{P+1})(\xi = -1)\\ &\quad= \phi(1) - \frac{1}{2^{P+1}}\prod_{q=1}^{P+1}(1 - \xi_q) - \phi(-1) + \frac{1}{2^{P+1}}\prod_{q=1}^{P+1}(-1 - \xi_q)\\ &\quad= 1 + \frac{1}{2^{P+1}}\left((-1)^{P+1}\prod_{q=1}^{P+1}(1 + \xi_q) - \prod_{q=1}^{P+1}(1 - \xi_q)\right)\\ &\quad= 1 + \frac{1}{2^{P+1}}\left((-1)^{P+1} - 1\right)\prod_{q=1}^{P+1}(1 - \xi_q), \qquad \text{(A.2)}\end{aligned}$$

where we have used the symmetry assumption on the set of points,

$$\prod_{q=1}^{P+1}(1 + \xi_q) = \prod_{q=1}^{P+1}(1 - \xi_q). \qquad \text{(A.3)}$$

Similarly, we can obtain an error estimate for the derivative in Lagrange interpolation,

$$\begin{aligned}&\frac{d\phi}{d\xi}(\xi_p) - \frac{d(\mathcal{P}\phi)}{d\xi}(\xi_p) \qquad \text{(A.4)}\\ &\quad= \frac{1}{(P+1)!}\left[\frac{\partial^{P+2}\phi}{\partial\xi^{P+2}}(\xi_p)\prod_{q=1}^{P+1}(\xi_p - \xi_q) + \frac{\partial^{P+1}\phi}{\partial\xi^{P+1}}(\xi_p)\sum_{r=1}^{P+1}\prod_{\substack{q=1\\q\neq r}}^{P+1}(\xi_p - \xi_q)\right]\\ &\quad= \frac{1}{(P+1)!}\frac{\partial^{P+1}\phi}{\partial\xi^{P+1}}(\xi_p)\prod_{\substack{q=1\\q\neq p}}^{P+1}(\xi_p - \xi_q)\\ &\quad= \frac{1}{2^{P+1}}\prod_{\substack{q=1\\q\neq p}}^{P+1}(\xi_p - \xi_q)\end{aligned}$$

for $p = 1, 2, \ldots, P+1$. Rearranging terms and substituting $\frac{d\phi}{d\xi}(\xi_p) = \frac{P+1}{2}\left(\frac{1+\xi_p}{2}\right)^P$ into (A.4) yields the desired identity. ∎

Proof of Lemma 3.3. Proceeding as in the proof of Lemma 3.1, let $j = P+1$ in (3.23). Then using the properties in (3.24)–(3.26) and Lemma 3.2,

$$\begin{aligned}
\boldsymbol{v}_{P+1} &= \frac{1}{(P+1)!}\left((1-\alpha)\boldsymbol{g_{L,\xi}} - \alpha\boldsymbol{g_{R,\xi}}\right)\left((\mathcal{P}s^{P+1})(\xi=1) - (\mathcal{P}s^{P+1})(\xi=-1)\right) \\
&\quad + \frac{1}{(P+1)!}\frac{d(\mathcal{P}s^{P+1})}{d\xi}(\boldsymbol{\xi}) - \frac{1}{2P!}\boldsymbol{s}^P \\
&\quad + \sum_{m=1}^{P+1}\frac{(-1)^m}{m!(P+1-m)!}(1-\alpha)\boldsymbol{g_{L,\xi}} + \frac{1}{(P+1)!}\alpha\boldsymbol{g_{R,\xi}} \\
&= \frac{1}{(P+1)!}\left((1-\alpha)\boldsymbol{g_{L,\xi}} - \alpha\boldsymbol{g_{R,\xi}}\right)\left(1 + \frac{1}{2^{P+1}}\left((-1)^{P+1}-1\right)\prod_{q=1}^{P+1}(1-\xi_q)\right) \\
&\quad + \frac{P+1}{2(P+1)!}\boldsymbol{s}^P - \frac{1}{2^{P+1}(P+1)!}\boldsymbol{\theta} - \frac{1}{2P!}\boldsymbol{s}^P \\
&\quad + \sum_{m=1}^{P+1}\frac{(-1)^m}{m!(P+1-m)!}(1-\alpha)\boldsymbol{g_{L,\xi}} + \frac{1}{(P+1)!}\alpha\boldsymbol{g_{R,\xi}} \\
&= \frac{1}{(P+1)!}\Bigg[\left((1-\alpha)\boldsymbol{g_{L,\xi}} - \alpha\boldsymbol{g_{R,\xi}}\right)\left(1 + \frac{1}{2^{P+1}}\left((-1)^{P+1}-1\right)\prod_{q=1}^{P+1}(1-\xi_q)\right) \\
&\quad - \frac{1}{2^{P+1}}\boldsymbol{\theta} - \left((1-\alpha)\boldsymbol{g_{L,\xi}} - \alpha\boldsymbol{g_{R,\xi}}\right)\Bigg] \\
&= \frac{1}{2^{P+1}(P+1)!}\Bigg[\left((1-\alpha)\boldsymbol{g_{L,\xi}} - \alpha\boldsymbol{g_{R,\xi}}\right)\left((-1)^{P+1}-1\right)\prod_{q=1}^{P+1}(1-\xi_q) - \boldsymbol{\theta}\Bigg],
\end{aligned}$$

where

$$\boldsymbol{\theta} = \left(\prod_{\substack{q=1\\q\neq p}}^{P+1}(\xi_p - \xi_q)\right)_{p=1,2,\ldots,P+1}. \tag{A.5}$$

Simplifying in the case of odd and even P,

$$-2^{P+1}(P+1)!\,\boldsymbol{v}_{P+1} = \begin{cases} \boldsymbol{\theta} & \text{odd } P, \\ 2\left((1-\alpha)\boldsymbol{g_{L,\xi}} - \alpha\boldsymbol{g_{R,\xi}}\right)\prod_{q=1}^{P+1}(1-\xi_q) + \boldsymbol{\theta} & \text{even } P. \end{cases} \tag{A.6}$$

Since $\boldsymbol{\theta} \neq \boldsymbol{0}$, it is certain that $\boldsymbol{v}_{P+1} \neq \boldsymbol{0}$ for odd P which proves the first half of the lemma. However, in the case of even P, if and only if

$$\left((1-\alpha)\boldsymbol{g_{L,\xi}} - \alpha\boldsymbol{g_{R,\xi}}\right)\prod_{q=1}^{P+1}(1-\xi_q) = -\frac{1}{2}\boldsymbol{\theta}, \tag{A.7}$$

then $\boldsymbol{v}_{P+1} = \boldsymbol{0}$ and the second part of the lemma is proven as well. ∎

Proof of Lemma 3.4. For the case of $P = 0$, the single solution point is located at the origin, $\boldsymbol{\xi} = [0]$, and the only correction functions that respect the boundary

constraints are given by $g_L(\xi) = \frac{1}{2}(1-\xi)$, $g_R(\xi) = \frac{1}{2}(1+\xi)$, so that $\boldsymbol{g_{L,\xi}} = [-\frac{1}{2}] = -\boldsymbol{g_{R,\xi}}$. The monomial $s^j(\xi)$ is approximated by its constant interpolant through $\xi = 0$, i.e., $(\mathcal{P}s^j) = \frac{1}{2^j}$. This yields

$$(\mathcal{P}s^j)(\xi = 1) = \frac{1}{2^j}, \quad (\mathcal{P}s^j)(\xi = -1) = \frac{1}{2^j}, \quad \frac{d(\mathcal{P}s^j)}{d\xi} = 0. \tag{A.8}$$

Proceeding as in the proof of Lemma 3.3, for any $j \geq 1$,

$$\begin{aligned}
v_j &= -\frac{1}{2(j-1)!}\frac{1}{2^{j-1}} + \sum_{m=1}^{j} \frac{1}{m!(j-m)!}\left((-1)^m(1-\alpha)\frac{-1}{2} + \alpha\frac{1}{2}\right)\frac{1}{2^{j-m}} \\
&= -\frac{1}{2^j(j-1)!} - \frac{1}{2}\sum_{m=1}^{j} \frac{1}{m!(j-m)!}\left((-1)^m(1-\alpha) - \alpha\right)\frac{1}{2^{j-m}} \\
&= -\frac{1}{2^j(j-1)!} - \frac{1}{2}\left[\sum_{m=0}^{j} \frac{1}{m!(j-m)!}\left((-1)^m(1-\alpha) - \alpha\right)\frac{1}{2^{j-m}} - (1-2\alpha)\frac{1}{2^j j!}\right] \\
&= -\frac{1}{2^j(j-1)!} - \frac{1}{2j!}\left[(1-\alpha)\left(-1+\frac{1}{2}\right)^j - \alpha\left(1+\frac{1}{2}\right)^j - (1-2\alpha)\frac{1}{2^j}\right] \\
&= -\frac{1}{2^j(j-1)!} - \frac{1}{2^{j+1}j!}\left[(-1)^j - 1 + \left((-1)^{j+1} - 3^j + 2\right)\alpha\right] \\
&= -\frac{1}{2^{j+1}j!}\left[2j + (-1)^j - 1 + \left((-1)^{j+1} - 3^j + 2\right)\alpha\right]
\end{aligned}$$

so that

$$-2^{j+1}j!\, v_j = \begin{cases} 0, & j = 1, \\ 4 - 8\alpha, & j = 2, \\ 4 - 24\alpha, & j = 3, \end{cases} \tag{A.9}$$

which shows that $v_1 \equiv 0$, $v_2 = 0$ if and only if $\alpha = \frac{1}{2}$, and $v_3 \neq 0$ if $\alpha = \frac{1}{2}$. ∎

Proof of Theorem 3.5.

1. $P = 0$: The proof follows directly from Lemma 3.4 and (3.15).
2. Odd P: The proof follows directly from Lemmas 3.1 and 3.3 and (3.15).
3. Even P: In the case of even P, begin by noting that the right-hand side of (3.28) is symmetric with respect to p, i.e.,

$$\prod_{\substack{q=1 \\ q\neq p}}^{P+1}(\xi_p - \xi_q) = (-1)^P \prod_{\substack{q=1 \\ q\neq p}}^{P+1}(\xi_p - \xi_q) = \prod_{\substack{q=1 \\ q\neq P+2-p}}^{P+1}(\xi_{P+2-p} - \xi_q), \tag{A.10}$$

owing to the symmetry of the solution points and that P is even. Hence,

$$(1-\alpha)g_{L,\xi_p} - \alpha g_{R,\xi_p} - (1-\alpha)g_{L,\xi_{P+2-p}} + \alpha g_{R,\xi_{P+2-p}} = 0. \tag{A.11}$$

Also, from the symmetry of the correction functions, $g_{R,\xi_p} = -g_{L,\xi_{P+2-p}}$ for $p = 1, 2, \ldots, P+1$, so that

$$\begin{aligned}
&(1-\alpha)g_{L,\xi_p} - \alpha g_{R,\xi_p} - (1-\alpha)g_{L,\xi_{P+2-p}} + \alpha g_{R,\xi_{P+2-p}} \\
&\qquad = (1-\alpha)g_{L,\xi_p} + \alpha g_{L,\xi_{P+2-p}} - (1-\alpha)g_{L,\xi_{P+2-p}} - \alpha g_{L,\xi_p} \\
&\qquad = (1-2\alpha)(g_{L,\xi_p} - g_{L,\xi_{P+2-p}}).
\end{aligned} \tag{A.12}$$

From (A.11) and (A.12),

$$(1-2\alpha)(g_{L,\xi_p} - g_{L,\xi_{P+2-p}}) = 0, \tag{A.13}$$

which shows that either $\alpha = \frac{1}{2}$ or $g_{L,\xi_p} = g_{L,\xi_{P+2-p}} = -g_{R,\xi_p}$. The result then follows from substitution into (3.28). ∎

Proof of Lemma 3.6. As a continuation of the proof for Lemma 3.4, note that for $P = 0$ the differentiation operator is a scalar given by (3.16),

$$Q(kh;\alpha) = \frac{1}{2}\sum_{m=1}^{\infty} \frac{(ikh)^m}{m!}\left((-1)^{m+1}(1-\alpha)+\alpha\right).$$

Then, using (3.22) and (3.34), the Taylor expansion of $F(kh;\alpha^{(2)},\alpha^{(1)})$ can be written as

$$\begin{aligned}
F &= Q^{(2)}\sum_{j=1}^{\infty}(ikh)^j v_j(\alpha^{(1)}) + ik\frac{h}{2}\sum_{j=1}^{\infty}(ikh)^j v_j(\alpha^{(2)}) \\
&= \sum_{j=1}^{\infty}(ikh)^j\left(Q^{(2)}v_j(\alpha^{(1)}) + ik\frac{h}{2}v_j(\alpha^{(2)})\right) \\
&= \sum_{j=1}^{\infty}(ikh)^j\left(\frac{1}{2}\sum_{m=1}^{\infty}\frac{(ikh)^m}{m!}\left((-1)^{m+1}(1-\alpha^{(2)})+\alpha^{(2)}\right)v_j(\alpha^{(1)}) + ik\frac{h}{2}v_j(\alpha^{(2)})\right) \\
&= \frac{1}{2}\sum_{j=1}^{\infty}(ikh)^{j+1}\Bigg[v_j(\alpha^{(1)}) + v_j(\alpha^{(2)}) \\
&\quad + \sum_{m=2}^{\infty}\frac{(ikh)^{m-1}}{m!}\left((-1)^{m+1}(1-\alpha^{(2)})+\alpha^{(2)}\right)v_j(\alpha^{(1)})\Bigg] \\
&= \frac{1}{2}(ikh)^2\left(v_1(\alpha^{(1)}) + v_1(\alpha^{(2)})\right) \\
&\quad + \frac{1}{2}(ikh)^3\left(v_2(\alpha^{(1)}) + v_2(\alpha^{(2)}) + \left(\alpha^{(2)}-\frac{1}{2}\right)v_1(\alpha^{(1)})\right) \\
&\quad + \frac{1}{2}(ikh)^4\left(v_3(\alpha^{(1)}) + v_3(\alpha^{(2)}) + \frac{1}{6}v_1(\alpha^{(1)}) + \left(\alpha^{(2)}-\frac{1}{2}\right)v_2(\alpha^{(1)})\right) \\
&\quad + \mathcal{O}\left((kh)^5\right).
\end{aligned}$$

Substituting $v_1 = 0$, $v_2(\alpha) = 4 - 8\alpha$, and $v_3 = 4 - 24\alpha$ from (A.9), we get

$$\begin{aligned}
F = &\frac{1}{2}(ikh)^3\left(8(1-\alpha^{(1)}-\alpha^{(2)})\right) \\
&+ (ikh)^4\left(3 - 10\alpha^{(1)} - 10\alpha^{(2)} - 4\alpha^{(1)}\alpha^{(2)}\right) + \mathcal{O}\left((kh)^5\right),
\end{aligned}$$

which completes the proof. ∎

Proof of Theorem 3.7.

1. $P = 0$: The proof follows directly from Lemma 3.6 and (3.33).

2. For $P > 0$, define $\sigma = \min(\sigma^{(1),1} - 1, \sigma^{(1),2})$. Then, substituting (3.35) into (3.34) yields

$$\begin{aligned}\boldsymbol{F} &= \boldsymbol{Q}^{(2)} \sum_{j=\sigma^{(1),1}+1}^{\infty} (ikh)^j \boldsymbol{v}_j^{(1)} + ik\frac{h}{2} \sum_{j=\sigma^{(1),2}+1}^{\infty} (ikh)^j \boldsymbol{v}_j^{(2)} \\ &= (ikh)^{\sigma+2} \left[\sum_{j=\sigma^{(1),1}-1-\sigma}^{\infty} (ikh)^j \boldsymbol{Q}^{(2)} \boldsymbol{v}_j^{(1)} + \frac{1}{2} \sum_{j=\sigma^{(1),2}-\sigma}^{\infty} (ikh)^j \boldsymbol{v}_{j-1}^{(2)} \right]. \end{aligned} \tag{A.14}$$

Now, by definition, $\sigma \leq \sigma^{(1),1} - 1$ and $\sigma < \sigma^{(1),2}$. So, from the triangle inequality,

$$\lim_{kh\to 0} |\boldsymbol{F}| \leq c(g^{(1)}, g^{(2)}, \alpha^{(1)}, \alpha^{(2)})(kh)^{\sigma+2}. \tag{A.15}$$

The proof then follows from (3.33). ∎

Appendix B. Proofs of results in section 4.

Proof of Lemma 4.1. Plugging (4.4) and (4.5) into (4.3) and using the triangle inequality, the Euclidean vector norm of derivative error can be bounded as follows:

$$\begin{aligned}\|\boldsymbol{E}(kh; g, \alpha)\|_2 &\leq k\frac{h}{2} \sum_{p=1}^{P+1} |\lambda_p(kh) - 1||\beta_p(kh)| \\ &\leq k\frac{h}{2} \left[|\lambda_1(kh) - 1||\beta_1(kh)| + \sum_{p=2}^{P+1} (|\lambda_p(kh)||\beta_p(kh)| + |\beta_p(kh)|) \right] \\ &\leq k\frac{h}{2} \left[c_1^{\lambda}(kh)^{q_1^{\lambda}} \left(\sqrt{P+1} + c_1^{\beta}(kh)^{q_1^{\beta}} \right) + \sum_{p=2}^{P+1} \left(c_p^{\lambda\beta}(kh)^{q_p^{\lambda\beta}} + c_p^{\beta}(kh)^{q_p^{\beta}} \right) \right] \\ &\leq \max_{p=2}^{P+1} \left(\sqrt{P+1} c_1^{\lambda}, c_p^{(\lambda\beta)}, c_p^{\beta} \right) (kh)^{1+\min_{p=2}^{P+1}\left(q_1^{\lambda}, q_p^{\lambda\beta}, q_p^{\beta}\right)} \text{ as } kh \to 0. \end{aligned} \tag{B.1}$$

Now, for any finite P, the equivalence of vector norms [15] implies that

$$\begin{aligned}\max_{p=1}^{P+1} |E_p(kh; g, \alpha)| &= \|\boldsymbol{E}(kh; g, \alpha)\|_{\infty} \\ &\leq c_{\infty,2} \|\boldsymbol{E}(kh; g, \alpha)\|_2 \end{aligned} \tag{B.2}$$

for some constant $c_{\infty,2}$. The proof now follows from (3.15). ∎

Proof of Lemma 4.2. The rate of convergence of λ_1^2 can be obtained from (4.7) by observing that

$$|\lambda_1^2(kh) - 1| = |\lambda_1(kh) - 1||\lambda_1(kh) + 1| \leq 2c_1^{\lambda}(kh)^{q_1^{\lambda}} \text{ as } kh \to 0. \tag{B.3}$$

Similarly, the rate of convergence of $\lambda^2\beta$ can be obtained from (4.5) and (4.7),

$$|\lambda_p^2(kh)\beta_p(kh)| = \frac{|\lambda_p(kh)\beta_p(kh)|^2}{|\beta_p(kh)|} \leq \frac{(c_p^{\lambda\beta})^2}{c_p^{\beta}}(kh)^{2q_p^{\lambda\beta} - q_p^{\beta}} \text{ as } kh \to 0. \tag{B.4}$$

Now, plugging (B.3), (B.4), and (4.5) into (4.9) and using the triangle inequality, the Euclidean norm of error in the second derivative can be bounded as follows:

$$\begin{aligned}
\|\boldsymbol{F}(kh;g,\alpha)\|_2 &\le \frac{k^2h^2}{4}\sum_{p=1}^{P+1}|\lambda_p^2(kh)-1||\beta_p(kh)| \\
&\le \frac{k^2h^2}{4}\left[|\lambda_1^2(kh)-1||\beta_1(kh)| + \sum_{p=2}^{P+1}(|\lambda_p^2(kh)||\beta_p(kh)|+|\beta_p(kh)|)\right] \\
&\le \frac{k^2h^2}{4}\Bigg[2c_1^{\lambda}(kh)^{q_1^{\lambda}}\left(\sqrt{P+1}+c_1^{\beta}(kh)^{q_1^{\beta}}\right) \\
&\qquad + \sum_{p=2}^{P+1}\left(\frac{(c_p^{\lambda\beta})^2}{c_p^{\beta}}(kh)^{2q_p^{\lambda\beta}-q_p^{\beta}} + c_p^{\beta}(kh)^{q_p^{\beta}}\right)\Bigg] \\
&\le \max_{p=2}^{P+1}\left(2\sqrt{P+1}c_1^{\lambda}, \frac{(c_p^{\lambda\beta})^2}{c_p^{\beta}}, c_p^{\beta}\right)(kh)^{2+\min_{p=2}^{P+1}\left(q_1^{\lambda},2q_p^{\lambda\beta}-q_p^{\beta},q_p^{\beta}\right)} \qquad \text{(B.5)}
\end{aligned}$$

as $kh \to 0$. The proof now follows from (B.2) and (3.33). ∎

Proof of Theorem 4.3. From [6], we know that λ_p for $p \neq 1$ diverges in the limit of $kh \to 0$. Then, from $\pi_p(k,h) = iak\lambda(kh) + bk^2\lambda^2(kh)$, for a fixed k,

$$|\pi_p^{-1}(k,h)| \to 0, \quad p = 2,\dots,P+1 \ \text{ as } h \to 0. \qquad \text{(B.6)}$$

Moreover, using (4.4) and (B.3) the convergence rate of π_1 can be obtained as

$$\begin{aligned}
|\pi_1(k,h) - (iak - bk^2)| &\le |ak||\lambda_1(kh)-1| + |bk^2||\lambda_1^2(kh)-1| \\
&\le c(k,a,b)h^{q_1^{\lambda}} \ \text{ as } h \to 0 \qquad \text{(B.7)}
\end{aligned}$$

for some k-dependent constant c. This immediately yields

$$|1 - (iak - bk^2)\pi_1^{-1}(k,h)| \le \frac{c(k,a,b)}{|(iak-bk^2)|}h^{q_1^{\lambda}} \ \text{ as } h \to 0. \qquad \text{(B.8)}$$

Then, from the triangle inequality, the Euclidean norm of pointwise error in the nth element can be bounded using (4.13) as follows:

$$\begin{aligned}
\|e_u(\boldsymbol{x}_n)\|_2 &\le \sum_{p=1}^{P+1}\left|1-(iak-bk^2)\pi_p^{-1}(k,h)\right||\beta_p(kh)| \\
&\le \left|1-(iak-bk^2)\pi_1^{-1}(k,h)\right||\beta_1(kh)| + \sum_{p=2}^{P+1}|\beta_p(kh)| \\
&\le \frac{c(k,a,b)}{|(iak-bk^2)|}h^{q_1^{\lambda}}\left(\sqrt{P+1}+c_1^{\beta}(kh)^{q_1^{\beta}}\right) + \sum_{p=2}^{P+1}c_p^{\beta}(kh)^{q_p^{\beta}} \\
&\le C'(k,a,b,P)\, h^{\min_{p=2}^{P+1}\left(q_1^{\lambda},q_p^{\beta}\right)} \ \text{ as } h \to 0, \qquad \text{(B.9)}
\end{aligned}$$

where C' is some scheme and equation dependent constant. The proof is completed by observing that

$$\begin{aligned}\|e_u\|_{\ell^2(\Omega^\delta)} &= \left[\frac{1}{N(P+1)}\sum_{n=1}^{N}\sum_{p=1}^{P+1}|e_u(x_{n,p})|^2\right]^{1/2}\\ &= \left[\frac{1}{N(P+1)}\sum_{n=1}^{N}\|e_u(\boldsymbol{x}_n)\|_2^2\right]^{1/2}\\ &\leq \frac{C'(k,a,b,P)}{P+1}\,h^{\min\limits_{p=2}^{P+1}(q_1^\lambda,q_p^\beta)} \quad \text{as } h\to 0. \qquad \text{(B.10)}\end{aligned}$$

□

Acknowledgment. We are grateful to David Williams[1] for his detailed comments regarding this manuscript.

REFERENCES

[1] S. Adjerid, K. D. Devine, J. E. Flaherty, and L. Krivodonova, *A posteriori error estimation for discontinuous Galerkin solutions of hyperbolic problems*, Comput. Methods Appl. Mech. Engrg., 191 (2002), pp. 1097–1112.

[2] M. Ainsworth, *Dispersive and dissipative behaviour of high order discontinuous Galerkin finite element methods*, J. Comput. Phys., 198 (2004), pp. 106–130.

[3] M. Ainsworth, P. Monk, and W. Muniz, *Dispersive and dissipative properties of discontinuous Galerkin finite element methods for the second-order wave equation*, J. Sci. Comput., 27 (2006), pp. 5–40.

[4] D. N. Arnold, F. Brezzi, B. Cockburn, and L. D. Marini, *Unified analysis of discontinuous Galerkin methods for elliptic problems*, SIAM J. Numer. Anal., 39 (2002), pp. 1749–1779, doi:10.1137/S0036142901384162.

[5] K. Asthana and A. Jameson, *High-order flux reconstruction schemes with minimal dispersion and dissipation*, J. Sci. Comput., 62 (2015), pp. 913–944.

[6] K. Asthana, A. Jameson, S. Lele, and P. Pinsky, *Analysis and Design of Optimal Discontinuous Finite Element Schemes*, Ph.D. thesis, Stanford University, Stanford, CA, 2016.

[7] H. L. Atkins and B. Helenbrook, *Super-convergence of discontinuous Galerkin method applied to the Navier–Stokes equations*, in 19th AIAA Computational Fluid Dynamics Conference, 2009, AIAA 2009-3787.

[8] R. Becker, P. Hansbo, and M. G. Larson, *Energy norm a posteriori error estimation for discontinuous Galerkin methods*, Comput. Methods Appl. Mech. Engrg., 192 (2003), pp. 723–733.

[9] P. Castonguay, D. M. Williams, P. E. Vincent, and A. Jameson, *Energy stable flux reconstruction schemes for advection–diffusion problems*, Comput. Methods Appl. Mech. Engrg., 267 (2013), pp. 400–417.

[10] Y. Cheng and C.-W. Shu, *A discontinuous Galerkin finite element method for directly solving the Hamilton–Jacobi equations*, J. Comput. Phys., 223 (2007), pp. 398–415.

[11] Y. Cheng and C.-W. Shu, *Superconvergence and time evolution of discontinuous Galerkin finite element solutions*, J. Comput. Phys., 227 (2008), pp. 9612–9627.

[12] Y. Cheng and C.-W. Shu, *Superconvergence of discontinuous Galerkin and local discontinuous Galerkin schemes for linear hyperbolic and convection-diffusion equations in one space dimension*, SIAM J. Numer. Anal., 47 (2010), pp. 4044–4072, doi:10.1137/090747701.

[13] B. Cockburn, G. Kanschat, I. Perugia, and D. Schötzau, *Superconvergence of the local discontinuous Galerkin method for elliptic problems on Cartesian grids*, SIAM J. Numer. Anal., 39 (2001), pp. 264–285, doi:10.1137/S0036142900371544.

[14] B. Cockburn, G. E. Karniadakis, and C.-W. Shu, *The Development of Discontinuous Galerkin Methods*, Lect. Notes Comput. Sci. Eng. 11, Springer, Berlin, 2000, pp. 3–50.

[15] G. H. Golub and C. F. Van Loan, *Matrix Computations*, Johns Hopkins Stud. Math. Sci., Johns Hopkins University Press, Baltimore, MD, 2013.

[1] CFD Engineer, Computational Aerodynamic Optimization, Flight & Vehicle Technology, Boeing Research & Technology.

[16] H. T. Huynh, *A flux reconstruction approach to high-order schemes including discontinuous Galerkin methods*, in 18th AIAA Computational Fluid Dynamics Conference, 2007, AIAA 2007-4079.

[17] H. T. Huynh, *A reconstruction approach to high-order schemes including discontinuous Galerkin for diffusion*, in 47th AIAA Aerospace Sciences Meeting, 2009, AIAA 2009-403.

[18] A. Jameson and K. Ou, 50 *years of transonic aircraft design*, Prog. Aerosp. Sci., 47 (2011), pp. 308–318.

[19] O. A. Karakashian and F. Pascal, *A posteriori error estimates for a discontinuous Galerkin approximation of second-order elliptic problems*, SIAM J. Numer. Anal., 41 (2003), pp. 2374–2399, doi:10.1137/S0036142902405217.

[20] D. M. Williams, P. Castonguay, P. E. Vincent, and A. Jameson, *Energy stable flux reconstruction schemes for advection–diffusion problems on triangles*, J. Comput. Phys., 250 (2013), pp. 53–76.